72 pages 258

DAA/Ames

Semiannual Progress Report

for

Theoretical Research Program To Study Transition Metal Trimers and Embedded Clusters

January 1,1985 - June 30,1985

Cooperative Agreement No: NCC2-296

Period of Award: July 1,1984 - June 30,1987

Principal Investigator: Stephen P. Walch

Eloret Institute
1178 Maraschino Drive
Sunnyvale,CA 94087

The objective of this research is to study small transition metal clusters at a high level of approximation i.e. including all the valence electrons in the calculation and also including extensive electron correlation. Perhaps the most useful end result of these studies is the qualitative information about the electronic structure of these small metal clusters. This information includes the nature of the bonding e.g. whether the 4s or 3d electrons are involved in the bond orbitals and also can provide information about reactivity. The electronic structure studies of the small clusters are directly applicable to problems in catalysis. From comparison of dimers, trimers and possibly higher clusters it is possible to extrapolate the information obtained to provide insights into the electronic structure of bulk transition metals and their interaction with other atoms and molecules at both surface and interior locations.

Because of the numerous practical aplications of transition metals, small metal clusters are currently of considerable experimental interest, and some information is currently becomming available both from matrix ESR studies and from gas phase spectroscopy. Currently the ESR experiments provide information on the neutral molecules (e. g. spin state and orbital character of the radical orbital as well as limited geometric information such as whether the atoms are equivalent or inequivalent). The gas phase spectroscopic work in principle can provide more detailed information, but for trimers and larger clusters, only Cu_3 has been succesfully studied. The experimental difficulties arise because of the high density of electronic states for these molecules and because for the neutral molecules a mixture of clusters (i. e. monomer, dimer, and trimer etc.) are present in the molecular beam. Future experimental studies therefore will be made on the positive

ions of the metal trimers, since these molecules may be mass selected. Thus, the ESR experiments are being used to study the neutrals, and gas phase spectroscopy is expected to provide information on the positive ions; while theory can provide a link between these experiments, since it can study either neutrals or positive ions.

The studies in the past year have concentrated on the electronic structure of the transition metal trimers. Here detailed studies have been made of Sc_3 and Cu_3 which are the elements on the ends of the first transition row. Studies are also being carried out for the positive ions of the transition metal trimers to help the experimentalists in their gas phase spectroscopic studies. Calculations have also been started for Ti_3^+ and V_3^+ and these will be continued in the current grant year. Comparison of these calculations to those for Sc_3^+ provides very valuable insights into the bonding trends in these molecules, just as similiar studies for the transition metal dimers provided a simple picture of the electronic structure of these molecules. As a start in understanding the reactivity of these molecules, the interaction of Sc_3 with a H atom will be studied. Initially, very simple questions such as whether the H atom will bond to the 3d or 4s derived levels of Sc_3 will be considered.

The studies on reactivity are relevant to experimental studies by Smalley et. al. on the reactivity of H_2 with Nb clusters and studies at Argonne National Laboratory on the reactivity of Fe clusters.

The main topic of this report is the electronic structure studies for Sc_3 and Cu_3. Preprints of this work are included in the appendix and only a few of the major results are presented here.

For the Cu_3 molecule all-electron studies have been carried out for

the ^2E state arising from three $4s^13d^{10}$ Cu atoms. For equilateral triangle geometries(D_{3h}) the lowest state is found to be $^2E'$ arising from $4sa_1'^2 4se'^1$. The $^2E'$ state exhibits strong Jahn-Teller distortion, leading to $^2A_1$ (acute angle) and $^2B_2$ (obtuse angle) minima in C_{2v} symmetry. Here the $^2B_2$ minimum is a true minimum on the surface while the $^2A_1$ minimum is a saddle point connecting adjacent $^2B_2$ minima. This strong Jahn-Teller distortion is consistent with the observed ground state vibrational levels in the gas phase spectroscopic studies of Morse, Hopkins, Langridge-Smith, and Smalley. The $^2B_2$ minimum is also consistent with the observed ESR spectrum of Cu_3 in a matrix, which has been interpreted as an obtuse angle structure with most of the spin density on the end Cu atoms. A linear $^2\Sigma_u^+$ state is found to be 0.26 eV higher.

Calculated vertical excitation energies for Cu_3 indicate that the upper state in the transition studied by Morse et. al. should be $^2A_1'$ not $^2E''$. An alternative assignment based on a $^2A_1'$ upper state is shown to account for the pattern of allowed hot bands and this revised assignment has been accepted by the experimentalists.

Calculations have also being carried out for Sc_3 molecule. This system was selected for study because of the ESR studies of Weltner et.al. which establish that the ground state of Sc_3 is a doublet state with equivalent Sc atoms which implies pairing of the 3d electrons into bond pairs. The calculations are in agreement with experiment in that the doublet states are lower than the high spin states and the wavefunctions show very definite indications of 3d bonding. Three doublet states have been studied. The dominant configurations for these states are:

$$^2A_1' = 4s\sigma a_1'^2\ 4s\sigma e'^4\ 3d\sigma a_1'^1\ 3d\pi a_2''^2$$

$^2A_2'' = 4s\sigma a_1'^2\ 4s\sigma e'^4\ 3d\sigma a_1'^2\ 3d\pi a_2''^1$

$^2E' = 4s\sigma a_1'^2\ 4s\sigma e'^3\ 3d\sigma a_1'^2\ 3d\pi a_2''^2$

Based on a combination of the calculations and the ESR experiments it was concluded that the $^2A_2''$ state is the ground state of Sc_3. Calculations were also carried out for the Sc_3^+ molecule in order to assist the experimentalists in doing gas phase studies of this species.

The results of this work will be presented at several scientific meetings. Among these are a i) NATO workshop on "Ab-Initio Quantum Chemistry-The Challenge of Transition Metals", to be held in Strasbourg, France, Sept. 1985 (invited 30 minute talk) ii) 5th International Congress on Quantum Chemistry, to be held in Montreal, Canada (poster presentation), and iii) an ACS Symposium on "The Theory of Metal Metal Bonding" to be held in New York city, April 1986 (Invited Talk).

On 3d Bonding in the Transition Metal Trimers: The Electronic Structure of Sc_3 and Sc_3^+

Stephen P. Walch[a]

Eloret Institute
Sunnyvale,CA 94087

and

Charles W. Bauschlicher,Jr.

NASA Ames Research Center
Moffett Field,CA 94035

Abstract

CASSCF/CCI calculations are presented for the low-lying states of Sc_3 and Sc_3^+, and SCF/CI calculations are presented for the $^1A_1'$ state of Ca_3 arising from three ground state ($4s^2$) Ca atoms, all for equilateral triangle geometries. The calculations use effective core potentials, developed by Hay and Wadt, which replace the Ne core but include the 3s and 3p core levels along with the valence electrons in the calculations.

The bonding in Ca_3 arises by 4s→4p promotion and leads to a well depth of about 0.5 eV for R(Ca-Ca) = 7.5 a_0. For Sc_3 the 4s bonding is similiar to that in Ca_3, but the 3d electrons are also strongly bonding leading to a $^2A_2''$ ground state with a well depth of about 1.0 eV and R(Sc-Sc) = 5.75 a_0. The good 3d bonding orbitals (bonding between all three atoms) are $3da_2''$ derived from atomic $3d\pi''$ and $3da_1'$ derived from atomic $3d\sigma$, while $3d\pi'$ atomic orbitals lead to $3de'$ orbitals which are bonding between pairs of atoms, and the $3d\delta'$ and $3d\delta''$ derived levels are non-bonding. (Here the atomic symmetry is given with respect to an axis connecting the atom to the center of the molecule.) Based on the Sc_3 calculations and preliminary calculations on Ti_3^+, the bonding in V_3^+ and Cr_3^+ is also discussed.

[a]Mailing Address: NASA Ames Research Center, Moffett Field, CA 94035.

I. Introduction

Transition metals and transition metal(TM) compounds are currently of considerable interest because of their relevance to catalysis and to materials science problems such as hydrogen embrittlement and crack propagation in metals. In spite of such interest, progress in understanding the chemistry of TM molecules has been slow due to both experimental and theoretical difficulties. For a review of the current state of both theory and experiment for TM molecules the reader is referred to the review article by Weltner and Van Zee[1].

For the TM trimers most of the current experimental information comes from matrix ESR studies. Here the assumption is made that the electronic state observed in the matrix is the ground state of the molecule. These studies directly give the electronic spin state of the molecule and analysis of the hyperfine structure gives some information on the electronic distribution of the open shell orbital(s). In some cases limited geometric information can also be derived e.g. for Sc_3 all the Sc atoms are found to be equivalent thus implying an equilateral triangle geometry[2]. To date gas phase spectra have been obtained only for the copper trimer[3]. These spectra permit only a vibrational analysis and thus do not give detailed geometric information, but the vibrational analysis does indicate a Jahn-Teller distorted ground state and provides vibrational frequencies for an excited state at an excitation energy of about 2.3 eV.

Because of the large number of low-lying states expected for the TM trimers and because of the presence of other multimers, the resonant two-photon ionization experiments, which were successful for Cu_3, can not be used in general to study the remaining TM trimers, due to spectral

complexity. It is, however, possible to use mass spectroscopy to pre-select and focus the positive ions. Thus, it is likely that the gas phase work will yield information about the positive ions, while ESR work will focus on the neutrals. Theory can provide a link between these two classes of experiments, since it can be applied to both the neutrals and positive ions.

In this paper we discuss complete active space SCF[4]/ externally contracted[5] configuration interaction (CASSCF/CCI) calculations for the low-lying states of Sc_3 and Sc_3^+. We also compare the bonding in the Ca_3, Sc_3, and Cu_3[6] molecules. From this comparison we are able to predict general trends for the TM trimers, much as we observed for the TM dimers[7].

Section II discusses the qualitative features of the bonding in the TM trimers including predicted trends for other TM trimers. Section III discusses the basis sets and other technical details of the calculations. Section IV discusses the calculated results for Sc_3 and Sc_3^+ and compares the results to experiment. Finally, Section V presents the conclusions from this work.

II. Qualitative Discussion.

As with the TM dimers[7] the nature of the bonding in the TM trimers changes with position in the transition row. The two principle factors controlling the electronic structure are i)the relative (n+1)s and nd orbital sizes which control the contribution of (n+1)s and nd bonding and ii) the $(n+1)s^2nd^m \rightarrow (n+1)s^1nd^{m+1}$ excitation energy of the atom which controls the atomic configurations which are available for bonding. As discussed in ref. 7, the ratio $<r_{(n+1)s}>/<r_{nd}>$ increases monotonically from 2.03 for Sc to 3.36 for Cu. Thus, we expect that nd bonding will be more favorable for the Sc end of the row than for the Cu end of the row. For Sc the $4s^23d^1$ state of the atom is lowest with the $4s^13d^2$ state about 1.4 eV higher. This excitation energy decreases monotonically from Sc to Cr which has a $4s^13d^5$ ground state. For Mn, $4s^23d^5$ is again lowest due to the large exchange interaction associated with a half filled 3d shell, but as for the left half of the row, the excitation energy decreases monotonically from Mn to Cu, which has a $4s^13d^{10}$ ground state. Thus, we expect that the ground states for Cr_3 and Cu_3 will arise from the $4s^13d^{m+1}$ states, while for the Sc_3 molecule the ground state configuration will involve a compromise between possible better bonding arising from 4s→3d or 4s→4p promotion and the excitation energy involved. Moving from Sc_3 toward Cr_3 one expects more 4s→3d promotion as the $(n+1)s^2nd^m \rightarrow (n+1)s^1nd^{m+1}$ excitation energy decreases.

For Cu_3 the ground state of the atom is $4s^13d^{10}$ with the closed 3d shell contracted with respect to the 4s. Thus, the bonding in Cu_3 is found to involve mainly the 4s electrons[6], much like an alkali trimer. However, the 3d electrons are not inert since correlating them results in a decrease

in R Cu-Cu of about 0.30 a_0. The Mulliken populations for Cu_3 from a CI calculation at the optimal geometry for D_{3h} symmetry (the ground state geometry here is Jahn-Teller distorted but near equilateral triangle) are 4s=2.72, 4p=0.47, and 3d=29.80 in agreement with the qualitative picture above.

For Ca_3 the lowest atomic limit is for three ground state atoms (^1S or $4s^2$). SCF/CI calculations have been carried out for this limit for equilateral triangle geometries and lead to the potential curves given in Fig. 1. Here the SCF curve is repulsive, but the CI curve shows a weak bond (about 0.5 eV) at R Ca-Ca = 7.5 a_0. At this distance, the populations from the CI calculation are 4s=5.24, 4p=0.61, and 3d=0.15. At R Ca-Ca = 6.5 a_0, the populations are 4s=4.58, 4p=1.08, and 3d=0.33. These results indicate a significant amount of 4s → 4p promotion as well as some 4s→ 3d promotion for shorter R Ca-Ca. For Ca_3 this formation of sp hybrids apparently does not lead to strong bonding; however, the large 4p populations at smaller R indicate that the predominate bonding mechanism here is 4s→ 4p promotion, as compared to the Ca_2 molecule which does not show the large 4p population and where a large part of the bonding is due to Van der Waals terms arising out of the 4s→ 4p near degeneracy effect[8]. The larger importance of 4s → 4p promotion for the trimer as compared to the dimer probably results from the formation of three bonds for the trimer which compensates for the 4s → 4p promotion energy, while the dimer with only one bond can not compensate for the promotion energy. Similar results have been observed by Bauschlicher, Bagus, and Cox[9] for Be_4, Mg_4, and Ca_4.

For Sc_3 we find the low-lying states arise from two atomic limits i)

three ground state $4s^23d^1$ atoms and ii) two ground state $4s^23d^1$ atoms and one excited state $4s^13d^2$ atom. This is to be expected based upon the results for Sc_2[10],[11], where it was shown that the ground state arises from one atom in the $4s^23d^1$ state and one atom in the $4s^13d^2$ state. For both of these atomic limits the bonding involves 4s to 4p promotion leading to sp hybrid bonding from the 4s shell, in addition ii) also involves 4s→3d promotion leading to a 3d population of about 4.0. For Sc_3 the 3d orbitals also contribute to the bonding. Because of the smaller size of the 3d orbitals compared to the 4s orbitals the formation of 3d bonds results in a much shorter Sc-Sc distance in Sc_3 as compared to the Ca-Ca distance in Ca_3. This is shown in Figure 2 where one sees that the $^2E'$ state of Sc_3 has a minimum, for D_{3h} geometries, for R Sc-Sc= 5.5 a_0, while the Ca_3 potential curve is strongly repulsive at this distance. This result implies a strong bonding effect from the 3d shell; although, the size mismatch of the 4s and 3d orbitals results in repulsive 4s-4s interactions at the short R Sc-Sc distances needed for formation of good 3d-3d bonds, and results in only weak molecular bonding.

The two principle 3d bonding orbitals for Sc_3 are a_1' which arises from the $3d\sigma$ atomic orbitals and a_2'' which arises from the $3d\pi''$ atomic orbitals. The configurations of the low-lying states here are:

$^2A_1' = 4sa_1'^2\ 4se'^4\ 3da_1'^1\ 3da_2''^2$

$^2A_2'' = 4sa_1'^2\ 4se'^4\ 3da_1'^2\ 3da_2''^1$

$^2E' = 4sa_1'^2\ 4se'^8\ 3da_1'^2\ 3da_2''^2$

The populations, for CASSCF wavefunctions at equilateral triangle geometries with R Sc-Sc= 5.5 a_0, are: 4s=4.55, 4p=1.17, 3d=3.24, and 4f=0.04 for the $^2A_2''$ and 4s=3.89, 4p=1.24, 3d=3.83, and 4f=0.04 for the $^2E'$. Thus,

the wavefunctions contain a considerable admixture of 4p character in agreement with the discusssion above.

The $^2A_1'$ and $^2A_2''$ states, which arise from three ground state atoms are weakly repulsive at the CASSCF level, as for Ca_3, but are bound at the CI level. The $^2E'$ state, which arises from two ground state atoms and one excited state atom($4s^13d^2$), is bound at the CASSCF level only with respect to its asymptote but is also bound with respect to three ground state atoms at the CI level. The $^2E'$ state is calculated to be 0.1 eV above the $^2A_2''$ state, in agreement with the ESR results[2] which indicate a non Jahn-Teller distorted ground state, consistent with the calculated $^2A_2''$ ground state of Sc_3.

For Sc^+, the promotion energy $4s^13d^1 \rightarrow 3d^2$ is much less than $4s^23d^1 \rightarrow 4s^13d^2$ for Sc atom [12], thus, for Sc_3^+ one expects a higher 3d population to be favored, and the ground state of the ion is expected to be derived from the $^2E'$ state of the neutral. By analogy to Cu_3, where the 4se′ orbital is only weakly bound, the lowest state of Sc_3^+ arises by removal of one electron from the 4se′ orbital. This leads to a $^3A_2'$ state with the electronic configuration:

$^3A_2' = 4sa_1'^2\ 4se'^2\ 3da_1'^2\ 3da_2''^2$

This configuration also leads to higher-lying $^1E'$ and $^1A_1'$ states. Starting with the $^2A_1'$, and $^2A_2'$ states, removal of one electron from the 4se′ orbital leads to $^3E'$ and $^3E''$ states with the configurations:

$^3E' = 4sa_1'^2\ 4se'^3\ 3da_1'^1\ 3da_2''^2$

$^3E'' = 4sa_1'^2\ 4se'^3\ 3da_1'^2\ 3da_2''^1$

These states are at 0.58 eV and 0.66 eV respectively above the ground state of Sc_3^+.

We now consider what would be likely configurations for other TM trimers of the first transition row. As Z increases, there will not be enough good 3d bonding orbitals available to accomodate all the 3d electrons. This situation is analagous to the TM dimers, where the $3d\sigma_g$ and $3d\pi_u$ are good bonding orbitals and the $3d\delta_g$ are weak bonding orbitals. Thus, the TM dimers are able to accomodate six electrons in good bond orbitals. For Ti_2 the 3d orbital occupancy is $3d\sigma_g^2 3d\pi_u^4$. For V_2 the extra two electrons go into the weakly bonding $3d\delta_g$ orbitals leading to the configuration $3d\sigma_g^2 3d\pi_u^4 3d\delta_g^2$. Here the δ orbitals form one-electron bonds which do not contribute significantly to the bond strength. For Cr_2 the $3d\delta_g$ orbitals contain four electrons which is unfavorable and the binding energy in Cr_2 is less than in V_2. This is understandable since for weakly overlapping orbitals, one-electron bonds whose bonding terms vary with distance like the overlap(S) are more favorable than two electron bonds whose bonding terms vary with distance like S^2[10].

Next we consider the symmetries of the molecular orbitals derived from the five possible atomic 3d orbitals. Here we consider 3d functions on each atom where the sigma direction is along the axis connecting the given atom with the center of the molecule. These 3d functions are classified with respect to the above axis as $3d\sigma$, $3d\pi'$, $3d\pi''$, $3d\delta'$, and $3d\delta''$, where the primes denote symmetry with respect to the molecular plane. In the molecular symmetry $3d\sigma$ and $3d\delta'$ transform as a_1' and e', $3d\pi'$ transforms as a_2' and e', $3d\pi''$ transforms as a_2'' and e'', and $3d\delta''$ transforms as a_1'' and e''. In order to show the symmetry properties of the 3d derived orbitals, plots of molecular orbitals for the Ti_3 molecule arising from $3d\sigma$, $3d\pi'$, $3d\pi''$, and $3d\delta'$ are given in Fig. 3. As for the TM dimers, we find that

the $3d\sigma$, $3d\pi'$, and $3d\pi''$ atomic orbitals have moderate overlaps in the molecule and form the bonding orbitals, while the $3d\delta'$ and $3d\delta''$ orbitals have small overlaps and are essentially non-bonding. Here we see that the best bond orbitals are $3d\sigma a_1'$ and $3d\pi'' a_2''$, because these combinations of the atomic orbitals have no molecular nodal planes between pairs of atoms. These same atomic orbitals also lead to $3d\sigma e'$ and $3d\pi'' e''$ orbitals which contain one molecular nodal plane, and are thus not favorable as bonding orbitals. However,these orbitals are important correlating orbitals, since they introduce molecular nodal planes between pairs of atoms. The $3d\pi' a_2'$ orbital is anti-bonding with nodal planes between all pairs of atoms, while the $3d\pi' e'$ orbitals contain one molecular nodal plane and are thus less favorable than $3d\sigma a_1'$ or $3d\pi''$, but are still bonding between pairs of atoms. Finally, the $3d\delta$ orbitals remain very atomic like due to the small overlaps of these atomic orbitals. Thus, these orbitals are essentially non-bonding.

This ordering of the 3d molecular orbitals is consistent with the occupations of the low-lying states of Sc_3 where the $3d\sigma a_1'$ and $3d\pi'' a_2''$ orbitals are occupied. For the Ti atom, the $4s^1 3d^3$ state is at 0.81 eV compared to 1.44 eV for the corresponding excitation in Sc. Thus, for Ti_3 one expects $4s \rightarrow 3d$ promotion to be more important than for Sc_3. Preliminary calculations for Ti_3^+ indicate two important groups of states. The first group of states arises from two Ti atoms in the ground state and one Ti^+ in the $4s^1 3d^2$ state which gives a 3d population of about six. These states are high spin (spin=8) and have an R(Ti-Ti) of about 7.5 a_0 for equilateral triangle geometries. The second group of states has a 3d population of about seven. The wavefunctions for these states are characteristic of 3d bonding, and these states are stable at much shorter bondlengths R(Ti-Ti)

$= 5.0\ a_0$. One representative configuration from this group of states is:

$1^6A_1' = 4sa_1'^2\ 4se'^2\ 3d\sigma a_1'^2\ 3d\delta' a_1'^1\ 3d\pi'' a_2''^2\ 3d\delta' e'^2$

This configuration is similar to the $^3A_2'$ state of Sc_3^+ with the extra 3d electrons in $3d\delta'$ derived levels. Since the $3d\delta'$ levels have very small overlaps, they are non-bonding. An alternative configuration is:

$2^6A_1' = 4sa_1'^2\ 4se'^2\ 3d\sigma a_1'^2\ 3d\delta' a_1'^1\ 3d\pi'' a_2''^2\ 3d\pi' e'^2$

One might expect this configuration to be lower, since the $3d\pi' e'$ levels are bonding between pairs of atoms. However,this configuration involves atomic configurations with two electrons in the $3d\pi$ orbitals which is not favorable for the Ti atom and this intraatomic coupling effect leads to comparable energies for the two configurations.

For V_3 and Cr_3 one expects the lowest state to arise from the three atoms in the $4s^13d^{n+1}$ state. The low-lying configurations here are expected to arise from the $1^6A_1'$ configuration of Ti_3^+ by first adding electrons to the bonding $3d\pi' e'$ levels, and then adding electrons to the non-bonding $3d\delta''$ levels. This model would result in increased bonding for V_3^+ as compared to Ti_3^+, but no increase in bonding in going from V_3^+ to Cr_3^+. This trend is consistent with V and Cr having the largest bulk cohesive energies[13] for the first transition row.

Mn_3 with a $4s^23d^5$ atomic ground state is expected to be like Ca_3 with the bonding arising from 4s→4p promotion. For the remaining elements of the first transition row, we expect mainly 4s bonding arising from mixtures of the $4s^23d^n$ and $4s^13d^{n+1}$ atomic states with the 3d electrons high spin coupled. Note that we expect 3d bonding to become less favorable as the 3d orbitals contract relative to the 4s for increasing nuclear charge within the first transition row. There is some experimental evidence for this viewpoint

from ESR studies which show that while Mn_2 has a singlet ground state but low-lying high spin states[14], the ground state of Mn_5 is high spin (spin=25) corresponding to all the 3d electrons high spin coupled[14].

III. Calculational Details

While these calculations could have been carried out at the all-electron level, accurate effective core potentials (ECP's) have been developed by Hay and Wadt [15] which make it possible to eliminate the Ne core with very little loss of accuracy. Here the 3s and 3p core levels as well as the 4s, 4p, and 3d valence levels are included in the calculation. The inclusion of the entire n=3 shell in the valence space is necessary since the 3p and 3d orbitals have similar spatial extents, e.g. removing the entire Ar core has lead to collapse problems for ScO[16a].

The basis set used in the Sc_3 calculations is the basis set reported by Hay and Wadt except that the 4p like functions were replaced by Wachters'[17] 4p functions multiplied by 1.5 to make them suitable for describing 4s→4p correlation. The s and p basis sets were contracted (2111) based on the 3s and 3p atomic orbitals, respectively. Normally, one augments the 3d basis by the Hay diffuse 3d function[18]. However, here the most diffuse 3d function is 0.0812 compared to the Hay diffuse 3d of 0.0588. A diffuse function selected based on an even tempered criterion was tried but it had very little effect on the energy of either the $4s^23d^1$ or $4s^13d^2$ state of Sc atom and it was concluded that the valence basis set was sufficiently diffuse. In order to describe polarization of the 3d bonds a single set of 4f functions was added as a two term fit of an STO(ζ=1.6). The Slater exponent here was optimized from an all electron CISD calculation for the $4s^13d^2$ state of the atom. The final basis set is (5s5p5d2f)/[4s4p3d1f].

The Ca atom basis set was constructed in the same way as the Sc basis set and the Hay and Wadt ECP with the 3s and 3p included in the valence was used as for Sc. The 3d functions here were taken from the

work of Pettersson, Siegbahn, and Ismail[19]. The primitive basis set here is 5d which is contracted (311). No 4f basis functions were added to the basis set, since there are no occupied 3d orbitals. The final basis set is (5s5p5d)/[4s4p3d].

Several tests were carried out for the Sc basis set/ECP used here. Atomic SCF calculations using the ECP gave a $4s^2 3d^1 \rightarrow 4s^1 3d^2$ excitation energy of 1.01 eV compared to 1.03 eV from NHF. Also all-electron calculations on the $4s^1 4p^1 3d^1$ state of the Sc atom showed that multiplying the 4p exponents by 1.5 raised the energy of this state by only 0.03 eV; this result is important since we expect strong 4s→4p promotion in Sc_3. Molecular calculations were also carried out for ScO and Sc_2. The ScO results were in good agreement with the all-electron results reported by Pettersson, Wahlgren, and Gropen[16b]. The ECP calculations for the $^5\Sigma_u^-$ state of Sc_2 compared well with all-electron results[20] (errors of -.04 a_0, -18 cm^{-1}, and 0.00 eV for R_e, ω_e, and D_e, respectively).

CASSCF/CCI calculations were carried out for Sc_3. Here the active space in the CASSCF included those molecular orbitals derived from 4s, $3d\sigma$, and $3d\pi''$ atomic orbitals. This choice is based on the discussion in section II. While the 4p should in principle also be included in the active space these functions mainly contribute to the 4s→4p near degeneracy effect which may be adequately treated in a subsequent CI calculation. The above atomic orbitals lead to molecular orbitals of a_1' and e' from 4s, of a_1' and e' from $3d\sigma$, and of a_2'' and e'' from $3d\pi''$. This gives a CASSCF calculation of nine electrons in nine orbitals which is small enough that it was possible to do the full CASSCF calculation, i.e. no orbital occupation constraints are necessary. Calculations were carried out at this level in order to determine

the low-lying states. Subsequent calculations were then carried out with the number of electrons in a′ and a″ orbitals constrained to be the same as in the dominant configuration. While this constraint results in a very substantial reduction in the number of configurations, it has very little effect on the total energy.

The reference configurations for the CCI calculations included the dominant configurations involving correlation of the 3d derived levels. For the $^2A_2''$ state five reference configurations were used consisting of the SCF plus $3da_1' \rightarrow e'$ double excitations(two configurations) and interpair terms between $3da_1'$ and $3da_2''$(two configurations). For the $^2E'$ state seven reference configurations were used. These were the analagous configurations to the five for the $^2A_2''$ state plus the double excitations from $3da_2'' \rightarrow 3de''$(two configurations). The calculations were carried out using the MOLECULE[21]-SWEDEN[22] system of programs.

IV. Discussion.

Tables I and II give calculated CASSCF energies for Sc_3 and Sc_3^+, respectively, while these values are plotted in Figure 2. CCI calculations have also been run for the $^2A_2''$ and $^2E'$ states. These energies are given in Table III.

Table IV. gives SCF and SCF/CI energies for the Ca_3 molecule, while these values are plotted in Figure 1. For the Ca_3 molecule some checks were done on the size consistency problem. Here for D_{3h} geometries at R Ca-Ca $= 50.0\ a_0$, the supermolecule CI energy is 0.29 eV above the sum of the atom CI energies, while adding Davidson's correction[22] to the supermolecule CI energy leads to an energy 0.04 eV below the sum of the atom CI energies. These results indicate that Davidson's correction works well for

the six electron problem resulting from three $4s^2$ atoms. These results also indicate that the supermolecule plus Davidson's correction energy is well approximated as the sum of the atom CI energies and this approximation was used for the Sc_3 calculations.

From Figure 2 one sees that the $^2E'$ state has a minimum in the CASSCF curve near 5.5 a_0. This state is derived from two ground state Sc atoms($4s^23d^1$) and one excited state atom($4s^13d^2$). The $^2E'$ state is bound with respect to this excited atomic limit but is about 0.3 eV above the lowest atomic limit. The $^2A_2''$ and $^2A_1'$ states are slightly higher in energy in this region and also the CASSCF curve is repulsive as was the case for the Ca_3 SCF potential curve. The CCI potential curve for the $^2A_2''$ state is bound by about 1.0 eV for a D_{3h} geometry with R Sc-Sc= 5.75 a_0. An interesting feature of the $^2A_2''$ CCI curve is a pronounced shoulder in the short R region. This feature is due to a curve crossing with another state of the same symmetry possibly derived from the same atomic limit as the $^2E'$ state. The $^2E'$ CCI curve has a more normal shape and is calculated to be less than 0.1 eV above the $^2A_2''$ state.

The experimental ESR spectrum[2] is clearly due to Sc_3, based on the presence of the HFS lines and approximate intensity ratios expected for interaction with three equivalent Sc nuclei. From the magnitude of the nuclear HFS interaction it is concluded that the singly occupied orbital contains less than 3 % 4s character. These results are consistent with the calculated $^2A_2''$ ground state, since this state should have an equilateral triangle geometry and the singly occupied orbital is predominately 3d like. The $^2E'$ state should Jahn-Teller distort which would be inconsistent with equivalent Sc atoms. For Cu_3, which also has a $^2E'$ ground state and exhibits strong

Jahn-Teller distortion[6], the lowest Jahn-Teller distorted component of $^2B_2$ symmetry is stabilized in the matrix, leading to inequivalent Cu atoms[24]. However, the $^2E'$ state of Sc_3 may be only weakly Jahn-Teller distorted, since the 3d bonding orbitals favor equilateral triangle geometries. Thus, the $^2E'$ state could have equivalent Sc atoms if it were only weakly Jahn-Teller distorted and exhibits rapid pseudorotation. But even if the Sc atoms were equivalent, the $^2E'$ state would not be consistent with the ESR, since the singly occupied orbital is mainly of 4s-4p character. For these reasons we conclude that the the $^2A_2''$ state is the ground state of Sc_3.

Moskovits, DiLeila, and Limm[25] have carried out resonance Raman studies of Ar matrices containing Sc. They report vibrational frequencies at 246, 145, and 151 cm^{-1} which they assign to Sc_3. Upon warming, the two lower frequencies coalesce into one frequency at 150 cm^{-1}. This behavior is interpreted as the removal of a matrix induced assymetry in the Sc_3 molecule in the originally deposited matrix. As these authors point out, the assignment of these lines to Sc_3 is based on comparison to other systems where the carrier of the spectrum could be established by isotopic substitution, but that this is not possible for Sc_3, due to only one stable isotope of the Sc atom. We calculate symmetric stretch frequencies of 513 cm^{-1} for $^2A_2''$ and 204 cm^{-1} for $^2E'$. The large difference in force constants between these two molecular states probably results from the steeper inner wall for the $^2A_2''$ state as a result of the larger 4s population. Assuming that $^2A_2''$ is the ground state of Sc_3, as suggested by a combination of the ESR results and the computations, the large discrepancy between our calculated symmetric stretch frequency of 513 cm^{-1} and the experimental value of 246 cm^{-1} suggests that the experimentally observed frequencies

do not arise from a Raman transition which terminates in the $^2A_2''$ state. However, it is possible that the final state is $^2E'$. This would imply that the separation between $^2A_2''$ and $^2E'$ is very small. The presence of non-degenerate bending modes in the final state is consistent with the $^2E'$ state if it is only weakly Jahn-Teller distorted. The $^2E'$ state need not be thermally populated. However, if both the $^2A_2''$ and $^2E'$ state were thermally populated and the $^2E'$ state is only weakly Jahn-Teller distorted the ESR spectrum of the $^2E'$ state may be too broad to observe. For Raman transitions the $^2A_2''$ state is connected to $^2A_2''$, $^2E'$, or $^2E''$ states. Thus, we would not see a Raman transition to the $^2A_1'$ state, but would expect to see transitions to the $^2A_2''$ state. These would be expected to occur near 500 cm^{-1}, where broad absorption is observed[25].

The lowest state of Sc_3^+ is a $^3A_2''$ state which has the configuration:

$^3A_2'' = 4sa_1'^2\ 4se'^2\ 3da_1'^2\ 3da_2''^2$

This state may be derived from the $^2E'$ state by removal of one electron from the 4se′ orbital. For the positive ion the 3d shell is expected to be stabilized with respect to the 4s shell; thus, a configuration with a 3d population near 4.0 is more stable for the positive ion, while for the neutral a state with a 3d population near 3.0 is more stable. Based on the CASSCF results, the ionization potential for removal of one electron from the 4se′ orbital of the $^2E'$ state is about 3.8 eV.

V. Conclusions.

CASSCF/CCI calculations have been presented for Sc_3 and Sc_3^+. The calculations use a [4s4p3d1f] basis set in conjunction with an effective core potential, developed by Hay and Wadt, which replaces the Ne core but includes the 3s and 3p core levels along with the valence electrons in the

calculations. Molecular tests of the Sc basis set and ECP used here indicate results in good agreement with all electron calculations.

The bonding in the lowest state of Sc_3 is found to arise from the three ground state($4s^2 3d^1$) atoms. The 4s bonding involves 4s → 4p promotion leading to 4s-4p populations of 4s = 4.55 and 4p = 1.17. The promotion energy involved is compensated for by the formation of three metal-metal bonds; thus, this bonding mechanism is favorable for the trimer but not for the dimer. The 3d electrons pair up to give a doublet ground state in agreement with the experimental ESR results. The low-lying states of Sc_3 have the configurations:

$^2A_1' = 4sa_1'^2\ 4se'^4\ 3da_1'^1\ 3da_2''^2$

$^2A_2'' = 4sa_1'^2\ 4se'^4\ 3da_1'^2\ 3da_2''^1$

$^2E' = 4sa_1'^2\ 4se'^3\ 3da_1'^2\ 3da_2''^2$

The $^2E'$ state dissociates to two ground state atoms and one excited state atom, while the other two states dissociate to three ground state atoms.

The ground state is assigned as $^2A_2''$ based on a combination of the calculations and ESR experiments, but the $^2E'$ state is very low-lying . The calculated symmetric stretch frequencies for the $^2A_2''$ and $^2E'$ states are 513 cm^{-1} and 204 cm^{-1}, respectively.

The lowest state of Sc_3^+ is a $^3A_2''$ state which has the configuration:

$^3A_2'' = 4sa_1'^2\ 4se'^2\ 3da_1'^2\ 3da_2''^2$

This state may be derived from the $^2E'$ state by removal of one electron from the 4se' orbital. For the positive ion the 3d shell is expected to be stabilized with respect to the 4s shell; thus, a state with a 3d population near 4.0 is lower for the positive ion, while for the neutral a state with a 3d population near 3.0 is lower.

ACKNOWLEDGMENTS

S.P. Walch was supported by a NASA grant(NCC2-296). We would like to acknowledge helpful discussions with Dr. Paul S. Bagus, Prof. Bill Weltner, and Dr. Richard VanZee. We would also like to thank Drs. P. J. Hay and W. R. Wadt for making their effective core potentials available to us prior to publication.

REFERENCES

1. W. Weltner,Jr., and R.J. VanZee, Ann. Rev. Phys. Chem., **35**, 291 (1984).
2. L.B. Knight,Jr., R.W. Woodward, R.J. VanZee, and W. Weltner,Jr., J. Chem. Phys., **79**, 5820 (1983).
3. M.D. Morse, J.B. Hopkins, P.R.R. Langridge-Smith, and R.E. Smalley, J. Chem. Phys., **79**, 5316(1983)
4. P. E. M. Siegbahn, A. Heiberg, B. O. Roos, and B. Levy, Physica Scripta, **21**, 323 (1980); B. O. Roos, P. R. Taylor, P. E. M. Siegbahn, Chem. Phys, **48**, 157 (1980); P. E. M. Siegbahn, J. Almlof, A. Heiberg, and B. O. Roos, J. Chem. Phys., **74**, 2381 (1981).
5. P.E.M. Siegbahn, Int. J. Quantum Chem. **23**, 1869(1983).
6. S.P. Walch and B. C. Laskowski, to be published
7. S.P. Walch and C.W. Bauschlicher,Jr., in "Comparison of Ab Initio Quantum Chemistry with Experiment", edited by R.J. Bartlett, Reidel Publishing, in press
8. S.P. Walch, H. Partridge, and C.W. Bauschlicher,Jr., unpublished results
9. C.W. Bauschlicher,Jr., P.S. Bagus, and B.N. Cox, J. Chem. Phys., **77**, 4032(1982).
10. S.P. Walch and C.W. Bauschlicher,Jr., Chem. Phys. Lett., **94**, 290(1983).
11. S.P. Walch and C.W. Bauschlicher,Jr., J Chem. Phys., **79**, 3590(1983).
12. C.E. Moore, Atomic Energy Levels, Circular 467 (National Bureau of Standards, Washington, 1949)
13. Ref. bulk cohesion energies
14. C.A. Baumann, R.J. VanZee, S. Bhat, and W. Weltner,Jr., J. Chem. Phys., **74**, 6977 (1981); J. Chem. Phys, **78**, 190 (1983)
15. P.J. Hay, and W.R. Wadt, J. Chem. Phys., **82**, 299(1985).

16a. O. Gropen, U. Wahlgren, and L. Pettersson, Chem. Phys., **66**, 459(1982).

16b. L.G.M. Pettersson, U. Walgren, and O. Gropen, Chem. Phys., **80**, 7(1983).

17. A.J.H. Wachters, J. Chem. Phys., **58**, 4452 (1973).
18. P.J. Hay, J. Chem. Phys., **66**, 4377 (1977).

19. L.G.M. Pettersson, P.E.M. Siegbahn, and S. Ismail, Chem. Phys., **82**, 355(1983).

20. S.P. Walch, and C.W. Bauschlicher,Jr., J. Chem. Phys., **79**, 3590(1983).

21. J. Almlof, MOLECULE, a gaussian integral program.

22. P.E.M. Seigbahn, C.W. Bauschlicher,Jr., B. Roos, A. Hieberg, P. R. Taylor, and J. Almof, SWEDEN, a vectorized SCF MCSCF direct CI.

23. S.R. Langhoff and E.R. Davidson, Intern. J. Quantum Chem., **8**, 61(1974).

24. J.A. Howard, K.F. Preston, R. Sutcliffe, and B. Mile, J. Phys. Chem., **87**, 536(1983).

25. M. Moskovits, D.P. DiLella, and W. Limm, J. Chem. Phys., **80**, 626(1984).

Table I.CASSCF Energies for Sc_3 (Equilateral Triangle Geometries)

R(Sc-Sc)	$^2E'$	$^2A_1'$	$^2A_2''$
4.75	-137.83351	----------	----------
5.00	-137.85695	----------	-137.82927
5.25	-137.86828	-137.8516	-137.85275
5.50	-137.87083	-137.86332	-137.86572
5.75	-137.86750	-137.87093	-137.87286
6.00	-137.86063	----------	-137.87821

Table II. CASSCF Energies for Sc_3^+ (Equilateral Triangle Geometries)
8

R(Sc-Sc)	$^3A_2''$	$^3E'$	$^3E''$
5.00	-137.71671	----------	----------
5.25	-137.72811	-137.69792	-137.69379
5.50	-137.73042	-137.70911	-137.70612
5.75	-137.72665	-137.71456	-137.71212
6.00	-137.71903	-137.713	----------

Table III. CCI Energies for Sc_3 (Equilateral Triangle Geometries)

R(Sc-Sc)	$^2A_2''$	$^2E'$
5.00	-137.99087	----------
5.25	-138.01180	-138.02351
5.50	-138.02436	-138.02899
5.75	-138.03413	-138.02890
6.00	-138.01591	-138.02570

Table IV. SCF and SCF/CI Energies for Ca_3 (Equilateral Triangle Geometries)

R(Ca-Ca)	SCF	SCF/CI
6.00	-108.57141	-108.69048
6.50	-108.60954	-108.72454
7.00	-108.62878	-108.74015
7.50	-108.63768	-108.74544
8.00	-108.64148	-108.74566
8.50	-108.64300	-108.74390
50.0	-108.64304	-108.73066

Figure 1. Calculated potential curves for the Ca_3 molecule for equilateral triangle geometries. The calculated binding energy for SCF and SCF/CI calculations is plotted as a function of R(Ca-Ca).

Figure 2. Calculated potential curves for selected states of Sc_3 and Sc_3^+ for equilateral triangle geometries. As for Fig. 1 the binding energy is plotted as a function of R(Sc-Sc). The curves are from CASSCF calculations except for the $^2A_2''$ and $^2E'$ states where contracted CI curves are also shown. The zero of energy for Sc_3 is taken as the sum of three ground state Sc atoms, while for Sc_3^+ the zero of energy is two ground state atoms and one Sc^+ atom in the $4s^1 3d^1$ state.

Figure 3. Contour plots of selected orbitals for the $1^6A_1'$ state of Ti_3^+. The orbitals are plotted in the molecular plane except for the $3d\pi''$ orbitals which are plotted 1.0 a_0 above the molecular plane.

Figure 4. Contour plots of selected orbitals for the $1^6A_1'$ state of Ti_3^+. The orbitals are plotted in the molecular plane.

Fig. 1

CALCULATED POTENTIAL CURVES FOR Ca_3

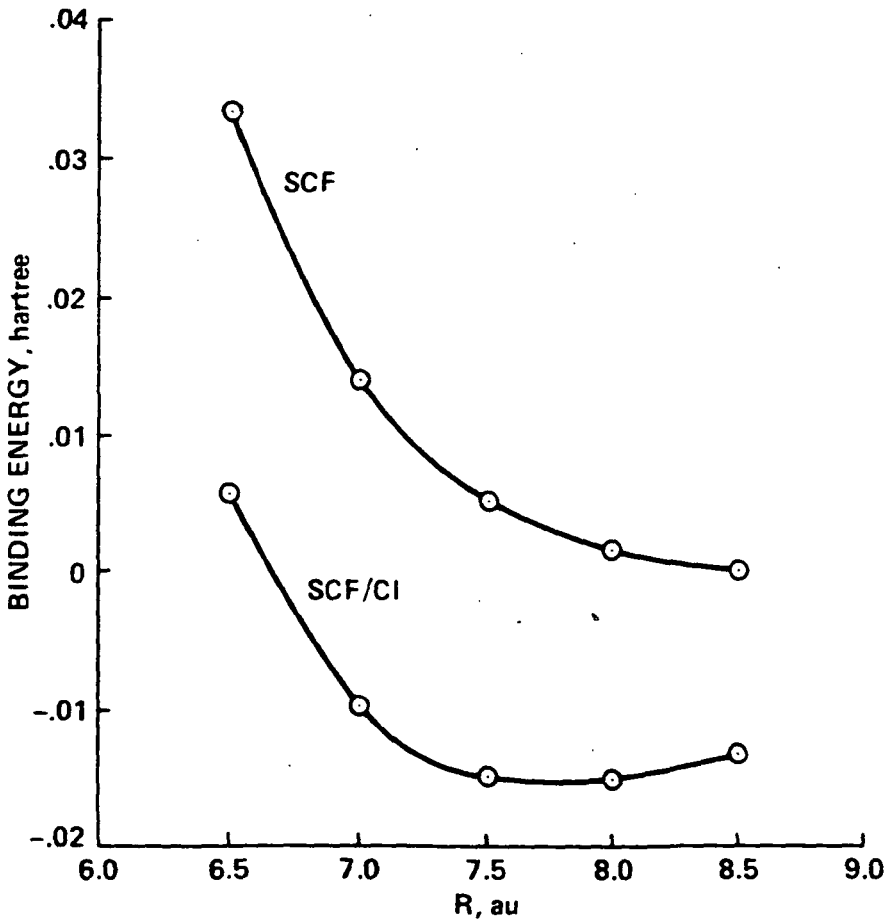

CALCULATED POTENTIAL CURVES FOR Sc_3 AND Sc_3^+

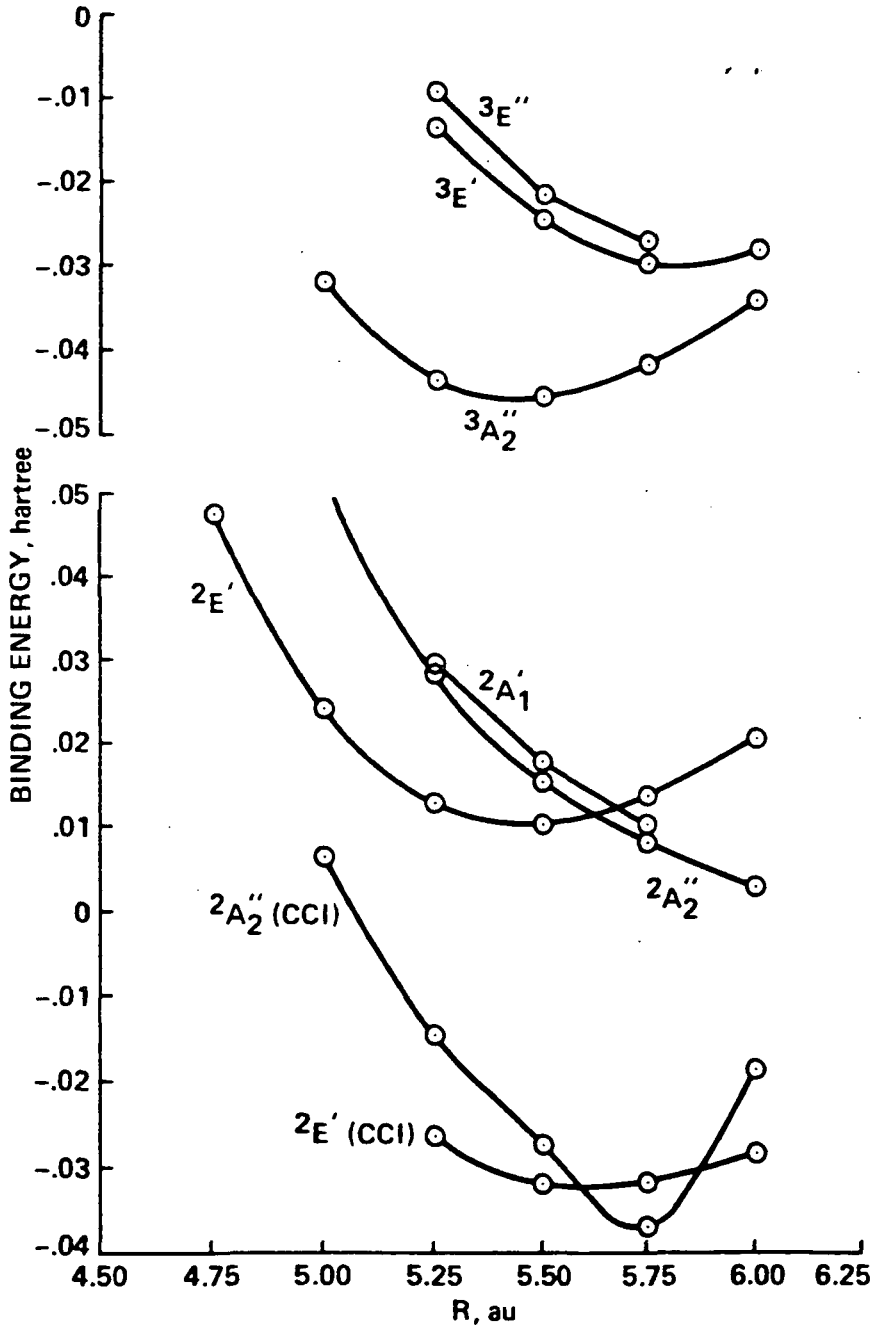

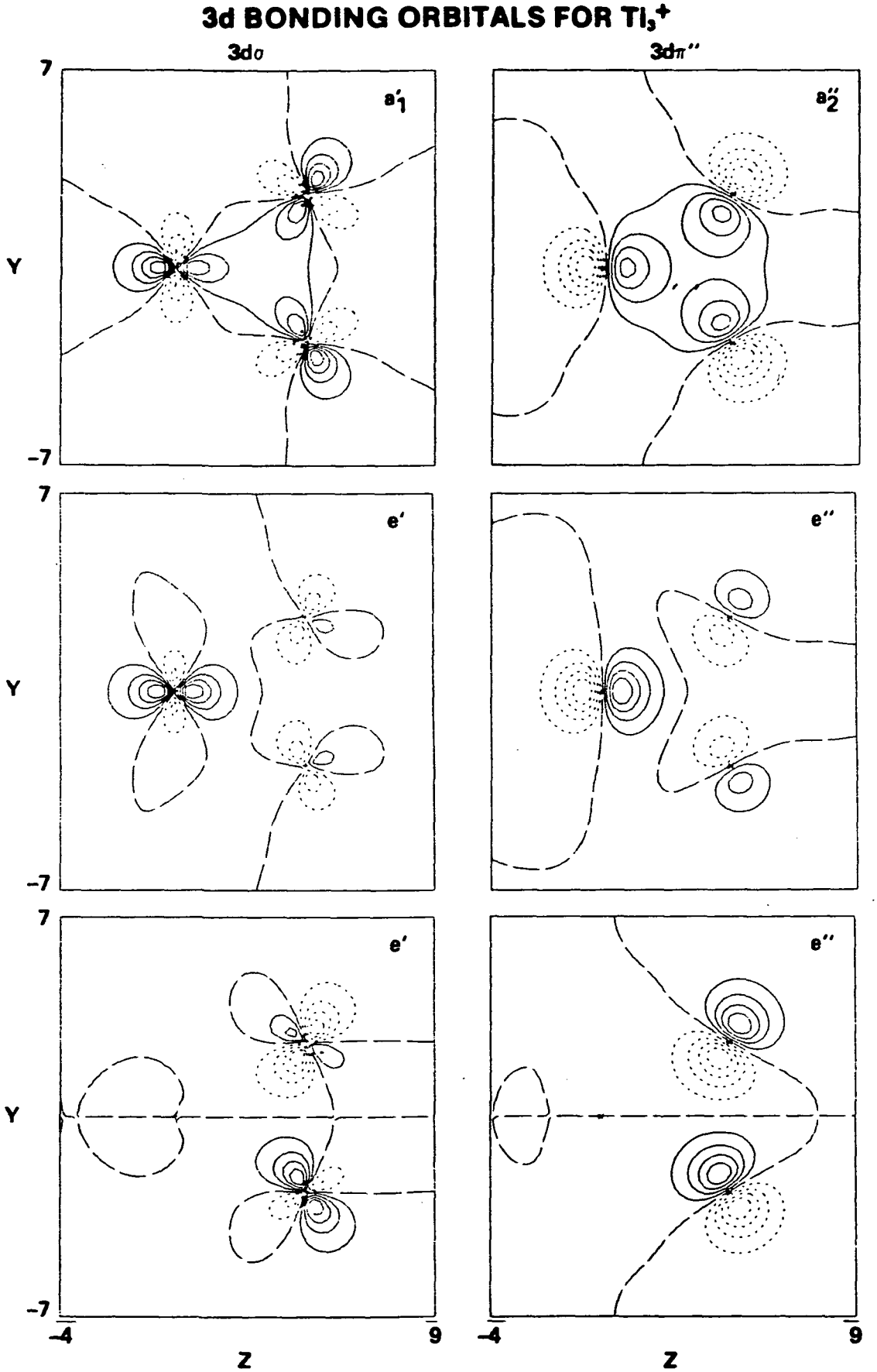
3d BONDING ORBITALS FOR Tl3+
3dσ
3dπ''
a'1
a''2
e'
e''
e'
e''
7
-7
Y
-4
9
Z

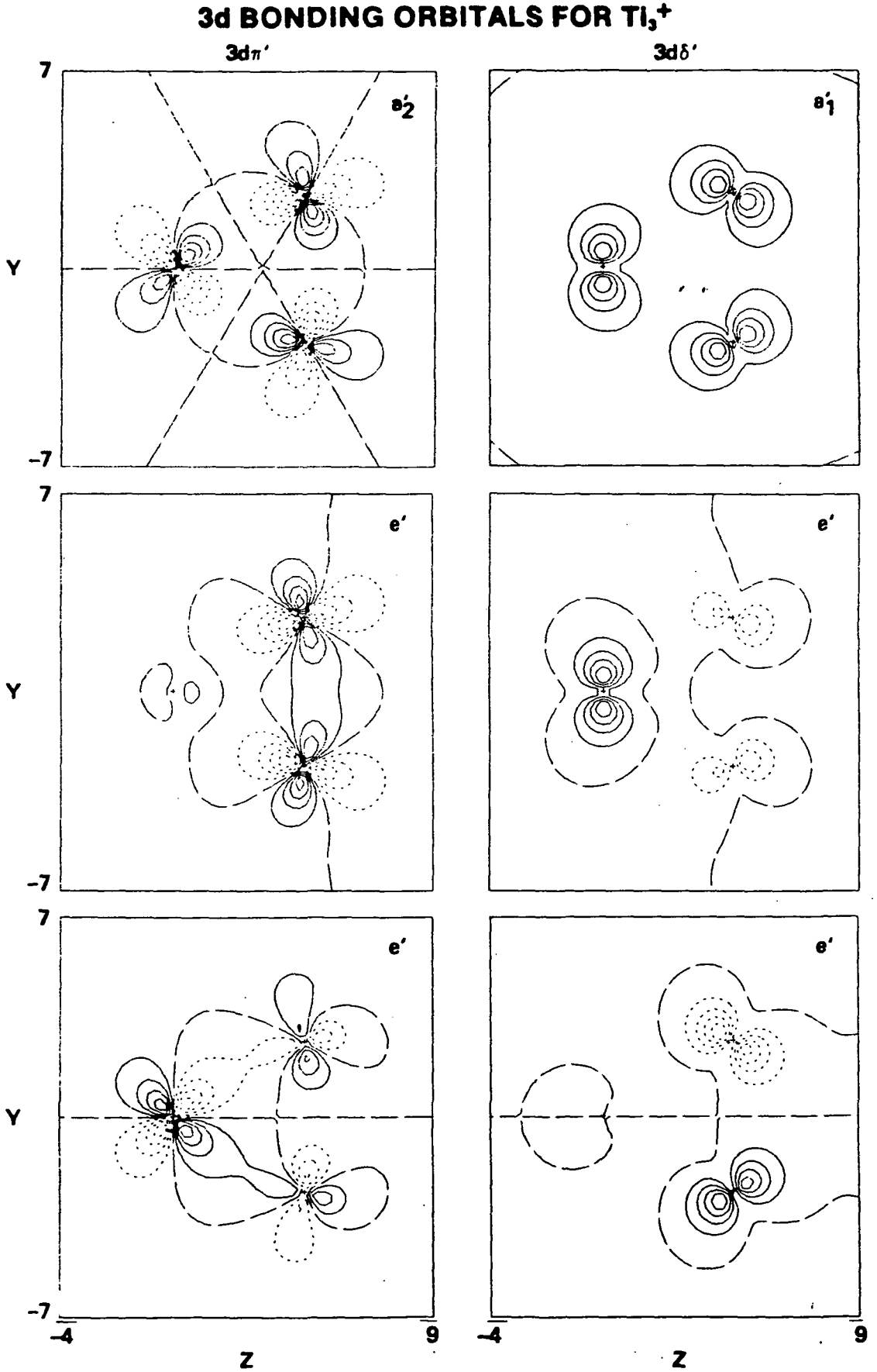
3d BONDING ORBITALS FOR Ti_3^+
3dπ'
3dδ'
a'2
a'1
e'
e'
e'
e'
e'
7
-7
Y
-4
9
Z

Calculated Ground State Potential Surface and Excitation Energies for the Copper Trimer

Stephen P. Walch[a]

Eloret Institute
Sunnyvale,CA 94087

and

Bernard C. Laskowski

Analatom Inc.[b]
Sunnyvale,CA 94089

Abstract

The results of an SCF/SDCI treatment are presented for selected portions of the ground state potential energy surface for the Cu_3 molecule. For equilateral triangle geometries(D_{3h}) the lowest state is $^2E'$ arising from $4sa_1'^2 4se'^1$. The $^2E'$ state exhibits strong Jahn-Teller distortion, leading to $^2A_1$ (acute angle) and $^2B_2$ (obtuse angle) minima in C_{2v} symmetry. Here the $^2B_2$ minimum is a true minimum on the surface while the $^2A_1$ minimum is a saddle point connecting adjacent $^2B_2$ minima. This strong Jahn-Teller distortion is consistent with the observed ground state vibrational levels in the gas phase spectroscopic studies of Morse, Hopkins, Langridge-Smith, and Smalley. The $^2B_2$ minimum is also consistent with the observed ESR spectrum of Cu_3 in a matrix, which has been interpreted as an obtuse angle structure with most of the spin density on the end Cu atoms. A linear $^2\Sigma_u^+$ state is found to be 0.26 eV higher.

Calculated vertical excitation energies for Cu_3 indicate that the upper state in the transition studied by Morse et. al. should be $^2A_1'$ not $^2E''$. An alternative assignment based on a $^2A_1'$ upper state is shown to account for the pattern of allowed hot bands.

[a]Mailing Address: NASA Ames Research Center, Moffett Field, CA 94035
[b]Mailing Address: Analatom Inc., 253 Humbolt Court, Sunnyvale, CA 94089

I. Introduction

Transition metals and transition metal(TM) compounds are currently of considerable interest, because of their relevance to catalysis and to materials science problems such as hydrogen embrittlement and crack propagation in metals. For a review of the current state of both theory and experiment for TM molecules, the reader is referred to the review article by Weltner and Van Zee[1]. Recent progress in the experimental characterization of TM molecules has come from both matrix isolation and gas phase spectroscopic approaches, while progress in the theoretical treatment of TM molecules has occurred as a result of improved methods of treating electron correlation. These improvements in part involve more efficient computational methods such as improved MCSCF[2],CASSCF[3], and direct CI[4] techniques, but also qualitative ideas such as the GVB[5] method have provided a conceptual framework for understanding electron correlation effects in these molecules.

For the transition metal trimers most of the current experimental information comes from matrix ESR studies. Here the assumption is made that the electronic state observed in the matrix is the ground state of the molecule. These studies directly give the electronic spin state of the molecule, and analysis of the hyperfine structure gives some information on the electronic distribution of the open shell orbital(s). In some cases limited geometric information can also be derived, e.g. for Sc_3 all the Sc atoms are found to be equivalent, thus implying an equilateral triangle geometry[6]. To date gas phase spectra have been obtained only for the copper trimer[7]. These spectra permit only a vibrational analysis and thus do not give detailed geometric information. However, the vibrational analysis

indicates a Jahn-Teller distorted ground state, and provides vibrational frequencies for an excited state at an excitation energy of about 2.3 eV. These new experimental results provide a challenge to theory to understand the bonding in the transition metal trimers.

There have been several previous all electron studies of the Cu_3 molecule [8,9,10]. SCF studies vary as to whether the linear geometry [8] or near equilateral triangle geometry [9] of Cu_3 are lowest, while CI studies [10] using a [2s1d] contracted basis set, which in effect eliminates most of the 3d shell correlation, place the distorted equilateral triangle structures lowest, but are not accurate enough to clearly establish the ground state geometry of this molecule. Diatomics in molecules (DIM) studies have also been reported for Cu_3 and other elements of group IB of the periodic table[11]. These studies also indicate a near equilateral triangle geometry for Cu_3. The present studies differ from previous studies in that larger basis sets and more extensive electron correlation are included in order to more accurately define the ground state surface. Additionally, calculations of the excited states are carried out in order to understand the resonant two photon ionization spectrum of Morse et. al. [7].

In order to understand the bonding in the copper trimer we first consider some features of the bonding in the copper dimer. Qualitatively, the bonding in Cu_2 has been described as a 4s-4s bond arising out of the $4s^13d^{10}$ ground state of the Cu atom[12]. Some controversy has arisen as to the role of the 3d electrons in this molecule[13]. While the $3d^{10}$ shell of Cu would reasonably be expected to remain atomic like since it is a closed shell and the 4s orbital is large with respect to the 3d orbital for Cu (The ratio $\langle r_{4s} \rangle$ / $\langle r_{3d} \rangle$ increases monotonically from 2.03 for Sc to 3.36

for Cu.[14]); the 3d electrons are not inert, since correlating them shortens the bond by 0.19 a_0. The resulting bond length is 0.15 a_0 longer than experiment; this error is found to result from about equal contributions from relativistic effects and higher excitations. Relativistic effects have been studied by Martin[15], by Scharf, Brode, and Ahlrichs[16], and by Werner and Martin[17],using all-electron treatments and by Laskowski et. al.[18] who have added relativistic effects using a relativistic ECP. These authors find a relativistic contraction of about 0.08 a_0. Studies of higher excitations by Martin[15], by Scharf, Brode, and Ahlrichs[16] and by Werner and Martin[17] using CEPA show that the remaining discrepancy is due to higher excitations. (Note that with two $3d^{10}$ shells of "spectator electrons" one expects a size consistency problem for Cu_2.) These studies indicate a need to correlate the 3d electrons in Cu_3. Indeed we find a substantial bond length contraction in Cu_3 due to correlating the 3d electrons. One also expects the same problems for Cu_3 as were observed for Cu_2 namely a relativistic contraction which would shorten the computed bond lengths and size consistency errors. Nonetheless, the non-relativistic SCF plus singles doubles CI model proved to be a useful model for Cu_2 and is expected to give the main features of the Cu_3 surface. In a related study Laskowski et. al.[18] have carried out calculations for the ground state surface of Cu_3 which incorporate relativistic effects using a relativistic ECP and use the CEPA method [19] to reduce the size consistency problem.

Starting with three $4s^13d^{10}$ Cu atoms and considering only the 4s electrons, leads to a $4sa_1'^2 4se'^1$ configuration for equilateral triangle geometries or a $^2E'$ state. The $^2E'$ state is a maximum on the potential surface with Jahn-Teller distortion leading to a splitting into $^2A_1$ (acute angle)

and $^2B_2$ (obtuse angle) minima in C_{2v} symmetry. Increasing the angle relative to the value for the $^2B_2$ minimum, leads to a gradual increase in the energy, and finally a linear geometry $^2\Sigma_u^+$ state which is calculated to be about 0.26 eV higher. In these calculations we concentrate on the C_{2v} cuts through the potential energy surface. These calculations lead to a calculated well depth (energy lowering for Jahn-Teller distortion of the ^2E state to the $^2B_2$ minimum) and barrier to pseudorotation (difference in energy between the $^2B_2$ minimum and the $^2A_1$ saddle point).

We also report calculations for the positive ion state ($4sa_1'^2$) of Cu_3 and for low-lying valence and Rydberg states. These calculations permit comparison to the experimentally measured ionization potential, and permit identification of the upper state in the transition reported by Morse, Hopkins, Langridge-Smith, and Smalley.[7]

Section II discusses the basis sets and other technical details of the calculations. Section III discusses the calculated potential surface for the $^2E'$ ground state of Cu_3. Section IV describes the calculations for the excited states of Cu_3. Finally Section V presents the conclusions from this work.

II. Calculational Details

The basis set used in these studies is essentially the Wachters' basis[20] for the ^2S state $4s^13d^{10}$ of the Cu atom. This basis set is augmented by the Wachters' 4p functions multiplied by 1.5 and the Hay diffuse 3d function[21]. The inner s and p functions are contracted in a segmented fashion using contraction III as recommended by Wachters, while the 4s and 4p functions are uncontracted, and the 3d functions are contracted (411) leading to an [8s6p3d] basis set. For Cu_2, addition of 4f functions to the

basis set decreased R_e by about 0.04 a_0 [12]. This is viewed as a small effect compared to the relativistic effects which are being neglected and these functions were not included here. The small importance of 4f functions for Cu_2 is a reasonable result given that the bonding involves mainly the 4s electrons of Cu, but is in contrast to results for those transition metal dimers which involve nd bonding where the 4f functions have a large effect [22,23,14].

For describing the excited states, it was necessary to add more diffuse basis functions, since most of the excited states are Rydberg like. The diffuse functions can be added either as atomic centered functions, in which case diffuse s and p functions are required on each Cu atom to describe s, p, and d Rydberg orbitals, or as molecule centered functions (at the molecular center), in which case s, p, and d functions are added. The latter approach has the advantage of requiring fewer basis functions, and also avoids linear dependency problems which can arise if very diffuse atomic centered functions are added. Three different basis sets were tried. The first, designated as diffuse(1), augmented the valence basis set with s, p, and d functions located at the molecular center, which were obtained as two term GTO fits(uncontracted)[24] to hydrogenic like STO 3s, 3p, and 3d functions (ζ=1/3). The diffuse(2) basis set was constructed like diffuse(1) except that a three term GTO fit was used, contracted (21), and one additional diffuse function of each type was added using an even tempered criterion. Finally, diffuse(3) was based on diffuse(2), but omitted the most diffuse set of molecule centered functions, and added one set of atom centered s and p diffuse functions obtained using an even tempered criterion. As discussed in section IV, the diffuse(1) basis set proved adequate

for describing the lowest six excited states of Cu_3(up to excitation energies of about 3.5 eV).

The integrals were computed in C_{2v} symmetry using MOLECULE[25]. The SCF calculations for the ground state surface were carried out in C_{2v} symmetry even for equilateral triangle geometries where higher symmetry could have been imposed. In the case of the calculations for the excited states which were restricted to equilateral triangle (D_{3h}) geometries, the higher symmetry was imposed. The SCF calculations were followed by singles and doubles CI. Here the high lying virtual orbitals corresponding to the antibonding combinations of the 1s, 2s, and 2p atomic levels were removed from the calculation. In general the 4s and 3d electrons were included in the calculation (33 electrons for Cu_3). In each case Davidson's correction[26] was computed and added to the computed CI energy, in order to include the main effects due to quadruple excitations. The SCF and CI calculations were carried out using the SWEDEN system of programs.[27]

III. The Ground State Surface

Table Ia shows energies for Cu_3 as a function of Cu-Cu distance for equilateral triangle geometries. From Table Ia one sees that CI leads to a bond length contraction for Cu_3 as was observed for Cu_2. Here the Cu-Cu bond length is 4.90 a_0 for SCF and 4.59 a_0 for CI, or a contraction of 0.31 a_0 compared to 0.21 a_0 for Cu_2. Table Ib shows similar information for Cu_3^+. From Tables Ia and Ib one sees that Cu_3 and Cu_3^+ have very similar symmetric stretching mode potential curves. The vibrational frequencies derived from the potential curves are 208 cm^{-1} for Cu_3 and 214. cm^{-1} for Cu_3^+. This result suggests that the 4se′ orbital of the ground state $4sa_1'^2 4se'^1$ configuration is non-bonding to slightly antibonding. (Note that

a difference of 6 cm^{-1} in vibrational frequency is not significant for the grid used here.) Since we identify the upper state in the transition observed by Morse et. al. [7] as a Rydberg state (See section IV.), it is appropriate to compare the computed Cu_3^+ frequency to the upper state symmetric stretch frequency of 243 cm^{-1}. The only other reported computed frequency for this state is 445 cm^{-1} from DIM calculations [11]. There is also an experimental value of 354 cm^{-1} by DiLella et. al. [28], but this experiment has been questioned by Morse et. al. [7] and by Weltner and Van Zee [1].

Tables II and III relate to the Jahn-Teller effect for the $^2E'$ state of Cu_3. These Tables show the variation in energy for the $^2A_1$ and $^2B_2$ symmetries as a function of Cu-Cu-Cu angle with two Cu-Cu distances fixed at 4.60 a_0. The same information is also presented graphically in Fig. 1. From Fig. 1 and Tables II and III, one sees that the $^2E'$ state is a maximum on the potential surface with distortion to C_{2v} symmetry leading to a lowering in the energy for both $^2A_1$ and $^2B_2$ symmetries. The $^2A_1$ symmetry favors acute angle geometries while the $^2B_2$ symmetry favors obtuse angle geometries. The $^2B_2$ surface shows a marked asymmetry leading at larger angles to a linear $^2\Sigma_u^+$ state. Table IV gives energies for linear geometries of Cu_3. This state is found to be about 0.26 eV higher than for the $^2B_2$ minimum.

Tables V and VI show the energies used in optimizing the geometries for the $^2A_1$ and $^2B_2$ structures in C_{2v} symmetry. The optimal geometries were derived via a two dimensional parabolic fit to the points given in the tables. From the optimal geometries given in Tables V and VI, one sees that the $^2B_2$ structure has two short Cu-Cu distances corresponding to two Cu-Cu bonds, while the $^2A_1$ structure has one short Cu-Cu distance and

two long Cu-Cu distances. From these geometric parameters one expects that the $^2A_1$ structure may be a saddle point interconnecting adjacent $^2B_2$ minima. This has been confirmed at the SCF level by elongating one of the long bonds and simultaneously contracting the other which leads to a decrease in the energy. The $^2B_2$ minimum on the other hand is expected to be a true minimum.

From the vibronic levels of the ground state, as obtained from analysis of the hot bands, Morse, Hopkins, Langridge-Smith, and Smalley[7] conclude that the ground state is strongly Jahn-Teller distorted. Following Herzberg [29], for an e′ vibration of a $^2E'$ electronic state, the vibrationless level is of $^2E'$ symmetry while the n=1 vibrational level leads to vibronic states of $^2E'$, $^2A_1'$, and $^2A_2'$ symmetry. For D_{3h} symmetry these levels are degenerate, but for a strong Jahn-Teller effect the levels are stabilized with the $^2A_1'$ and $^2A_2'$ levels still degenerate and below the $^2E'$ level (See Fig. 2). Our interpretation of the spectrum has the $^2A_1'$ and $^2A_2'$ levels 15 cm^{-1} above the vibrationless level, while the $^2E'$ level is 100 cm^{-1} above the vibrationless level.

Morse et. al.[7] have computed the $^2E'$ vibronic levels for a potential with a well depth of 543 cm^{-1} and a barrier height of 407 cm^{-1}. They find the $^2A_1'$ level to be only 2.8 cm^{-1} above the ground vibronic level, as compared to an experimental estimate of 15 cm^{-1}. The parameters calculated in the present work are a well depth of 555 cm^{-1} and a barrier height of 171 cm^{-1}. It would be interesting to see if these parameters would give better agreement with experiment.

The $^2B_2$ ground state is also consistent with the matrix ESR work of Howard, Preston, Sutcliff, and Mile [29], which has been interpreted as an

obtuse angle structure with most of the spin density on the end Cu atoms. Note that the observed spin density is consistent with a $^2B_2$ state, but not with a $^2A_1$ state which would have substantial spin density on the central Cu atom. For comparison we show in Table VII. the Mulliken populations for the singly occupied b_2 orbital for the $^2B_2$ state and the singly occupied a_1 orbital for the $^2A_1$ state. We should note here that the $^2A_1$ and $^2B_2$ states are calculated to be close in energy which is consistent with recent experimental results for Ag_3 by Kernisant, Thompson, and Lindsay [31], where it is shown that matrix effects invert the ordering of these states.

The calculated binding energies for the Cu_2 and Cu_3 clusters were obtained from the CI wavefunctions. Here size consistency problems introduce some uncertainty in the computed binding energies. For Cu_2 the supermolecule CI energy ($R_e = 50.$ a_0) is 0.45 eV above the sum of the Cu atom CI energies. This error results from the neglect of quadruple excitations which arise as products of double excitations from each of the Cu atom $3d^{10}$ shells. Including Davidson's correction leads to a supermolecule energy 0.34 eV below the sum of the atom CI energies. In these calculations we choose to compare the CI plus Davidson's correction energy near R_e with twice the singles doubles CI energy for the Cu atom. This procedure, while consistent in the level of excitation, may overestimate the binding energy due to the overestimation of the effect of quadruples in the molecular calculation by Davidson's correction. The resultant D_e is 1.93 eV compared to an experimental value of 2.05 eV[32]. For Cu_3 a reasonably consistent procedure is to compare the Cu_3 $^2B_2$ CI plus Davidson's correction energy to the Cu_2 CI plus Davidson's correction energy plus the Cu atom CI energy. Note that within the limits of the use of Davidson's correction, we are then compar-

ing CI through quadruples for each case. While hextuple excitations could contribute for the trimer, they are expected to be an order of magnitude less important than the quadruples. The resultant binding energy is 0.56 eV for Cu_3 relative to Cu_2 plus Cu atom, as compared to an experimental value of about 1.0 eV [33]. The larger error here may be due to neglect of hextuple excitations, and the indication is that single double excitation CI treatments will be less accurate as the cluster size increases.

A question which naturally arises is how accurate are the relative energies of the various structural isomers of Cu_3. The two major sources of error here are size consistency and basis set superposition error. The magnitude of the size consistency error can be judged from the effect on the R_e of Cu_2. Here size consistency effects are judged to make R_e too long by about 0.05 a_0; from this we conclude that higher excitations are more important as R Cu-Cu decreases. An estimate of the R dependence of this effect near R_e may be made from the Cu_2 SDCI potential curve. Here compressing the bond by 0.10 a_0 from R_e(the change in the potential curve necessary to reduce R_e by 0.05 a_0) increases the energy by 0.010 eV. Thus it would seem that for small changes in geometry, size consistency effects would not substantially distort the potential surface. The other potential problem is basis set superposition error. Here we calculate a CI superposition error of 0.06 eV for one atom due to the basis set on an adjacent atom, for $R = 4.5$ a_0 but relatively slow variation with small changes in distance near R_e. From the calculated CI basis set superposition error curve, we estimate an increase in the $^2B_2 \rightarrow {}^2A_1$ separation from 171 cm^{-1} to 223 cm^{-1} and a reduction in the equilateral triangle to linear separation from 0.26 eV to 0.14 eV. However, these effects will be

compensated for to some extent by the size consistency errors which have the opposite phase and are of the same order of magnitude. We conclude that a more complete basis set/CI calculation will still find equilateral triangle geometries below linear geometries and will find a small $^2B_2 \rightarrow {}^2A_1$ separation with $^2B_2$ lower. These conclusions have been confirmed by the results of Ref. 18 which show a smaller $^2B_2 \rightarrow {}^2A_1$ separation than in the present calculations and somewhat shorter Cu-Cu bond lengths (due to relativistic effects), but do not change any of the major features of the computed ground state surface. The excitation energies will not be effected by size consistency effects, since the ground state and excited state have similiar geometries and hence the size consistency error is constant.

Comparing now to other computed results, previous all-electron studies [8,9,10] did not include sufficient levels of electron correlation to clearly establish the features of the ground state surface. Although there was general agreement that the near equilateral triangle region of the surface displayed a strong Jahn-Teller effect and the $^2A_1$ and $^2B_2$ structures were close in energy, the relative energies of the near equilateral triangle geometries and linear geometries were not clearly established. DIM [11] studies, which incorporate some of these effects in a semiempirical fashion through the use of accurate potential curves for the diatomics, did lead to energetics in reasonable agreement with the present calculations. Here the equilateral triangle - linear separation is 0.18 eV in good agreement with our best estimate of 0.14 eV, and the Jahn-Teller stabilization energy is 480 cm^{-1} compared to 555cm—1 in our calculation. However, the computed symmetric stretch frequency is 445 cm^{-1}, which is much larger than our calculated value and, accepting our interpretation of the experiment, also much

larger than the experimental value of 243 cm^{-1}.

IV. Calculated Vertical Excitation Energies.

As discussed in section III, the ground state of Cu_3 for equilateral triangle geometries is $^2E'$, arising from a $4sa_1'^2 4se'^1$ configuration. From comparison of the calculated symmetric stretching frequencies of Cu_3 and Cu_3^+, we see that the 4se′ orbital is essentially nonbonding. Given this one expects that the low-lying excited states of Cu_3 will arise by excitation of a single electron from the 4se′ orbital to various virtual orbitals, while leaving the $4sa_1'^2$ configuration intact. This is equivalent to saying that the excited states formally have the character of Rydberg like states, since they correspond to a single electron in the field due to Cu_3^+. The solutions to such a problem are expected to be hydrogenic like. The excitation energies given in table VIII were obtained from a combination of a valence CI calculation, to determine which low-lying states exist and SCF plus singles and doubles CI calculations to determine the excitation energies. Because the excited states of Cu_3 are Rydberg like, a good approximation to the occupied orbitals is obtained from an improved virtual orbital(IVO) calculation[34], which in the present case is equivalent to a calculation on the positive ion. To determine the nature of the low-lying Rydberg states we carried out a valence CI calculation which consisted of full CI for the three valence electrons among the space of the bound virtual orbitals of the positive ion calculation. This calculation leads to the valence CI values in Table VIII. Subsequent SCF plus singles and doubles CI was carried out to determine the excitation energies.

Figure 3. shows selected valence and Rydberg orbitals for Cu_3 obtained from an SCF calculation for Cu_3^+. The 4se′ orbital which is occupied in

the ground state is like a hydrogenic 2p function. This is clearly a valence state since the 4se′ orbital is largely Cu 4s like. The other component of the hydrogenic 2p is an a_2'' orbital, which turns out to be of mixed valence Rydberg character. The lowest excited state of Cu_3 is a $^2A_2''$ state arising from this level. This excited state which occurs at 1.25 eV is not dipole allowed from the ground state of Cu_3 without vibronic coupling.

The remaining five excited states of Cu_3 which are reported here arise from singly occupied orbitals that have the character of n=3 hydrogenic levels, i.e. they exhibit Rydberg character. The assignment of these levels to n=3 is based on the effective quantum numbers obtained from the computed excitation energies and the computed ionization potential. These values are consistent with quantum defects of 0.8, 0.2-0.6, and 0.6 for 3s, 3d, and 3p hydrogenic levels, respectively. It should be noted here that the Rydberg n value has no relationship to the principle quantum number for the Cu atom. The geometries of these states are expected to be very similar to the geometry of Cu_3^+. From section III. we saw that both Cu_3 and Cu_3^+ have D_{3h} minima at nearly the same geometry (an equilateral triangle geometry with R Cu-Cu = 4.60 a_0). Table VIII shows the calculated vertical excitation energies for Cu_3 at the geometry given above. The electronic symmetries here are (with the Rydberg orbital character given in parenthesis) $^2A_1'(3sa_1')$, $^2E'(3de')$, $^2E''(3de'')$, $^2A_1'(3da_1')$, and $^2E'(3pe')$.

The excited states discussed so far arise only from the 4s derived levels of the Cu atom. Because the $4s^23d^9$ state of Cu atom is only 1.5 eV above the $4s^13d^{10}$ state it is possible that low-lying states may exist in which one Cu atom is in the $4s^23d^9$ excited state. Such states have been studied by

Walch and Goddard [35] for Ni_3. Here it is found that the central atom is $4s^23d^8$ while the end atoms are $4s^13d^9$. The central Ni atom forms sp hybrids directed at 180 degrees from each other. These sp hybrids then form bonds to the 4s orbitals of the end Ni atoms leading to a linear ground state. Similarly for Cu_3 we find the lowest state of this limit is a $^2\Delta$ state with the 3d hole localized on the central Cu atom (linear geometries). Table IX gives computed SCF/CI energies for linear geometries. The computed excitation energy is 1.63 eV and the best estimate of the excitation energy is 1.95 eV (correcting for the error in the $4s^13d^{10} \rightarrow 4s^23d^9$ excitation energy of the atom). This excitation energy is for the $^2\Delta$ state at the optimal linear geometry compared to the $^2B_2$ component of the ground state at its optimal geometry. Given the sharp bending curve for the analagous state of Ni_3 we expect that this state will be way above the 2.3 eV excitation energy in the transition studied by Morse et. al. [7] for equilateral triangle geometries. Additionally, the upper state in that transition has a geometry close to that of the ground state which essentially excludes linear states from consideration.

Morse et. al.[7] assign the upper state in the transition which they observe at about 2.3 eV as $^2E''$. This assignment is based on the presence of anharmonicity in the upper state vibrational levels in the normal mode interpretation, which can be explained by assuming that the upper state is weakly Jahn-Teller distorted; although, the upper state levels can also be fit to vibrational frequencies of 149 cm^{-1} and 252 cm^{-1} but with significant anharmonicities. The Jahn-Teller distorted upper state model requires either a $^2E'$ or $^2E''$ upper state. The choice of the $^2E''$ symmetry is consistent with the observation that one vibronic component of the ground

state ($^2A_1'$ or $^2A_2'$) is not radiatively coupled to the vibrationless level of the upper state. The Jahn-Teller distortion in the upper state is found to be very small corresponding to a Jahn-Teller stabilization energy of only 9 cm^{-1}. Our initial assumption was that the upper state was of $^2E''$ symmetry, and the small Jahn-Teller distortion was consistent with the Rydberg nature of the e'' orbital in this state. However, the calculated excitation energy to this state is 3.32 eV which is about 1.0 eV above the observed transition energy. After careful checks on the basis set(see below) we conclude that our excitation energy could not be in error by this much. Rather, we believe that the $^2A_1'$ state, which we calculate to be at 2.14 eV, is the upper state observed at about 2.3 eV. This state also turns out to be consistent with the selection rules observed for the hot bands.

Figure 2 shows the vibronic levels for the ground state of Cu_3 as expected for a strongly Jahn-Teller distorted molecule. The actual locations are obtained from analysis of the spectrum of Cu_3 as measured by Morse et. al.[7] (See Figure 4). The main feature of Figure 4 is a vibrational progression in the bending mode. Here the 0→0 band corresponds to band 2 and the remaining members of the progression are 5, 7, 9, and 12 (The vibrational frequency here is 146. cm^{-1}.). The strong origin band here is consistent with the similar geometries for the two states in the transition. The symmetric stretching mode corresponds to 243 cm^{-1}, and accounts for 6 and 10. The remaining bands 8 and 11 require anharmonicity corrections, but can be explained in a normal modes interpretation. A key remaining feature is the presence of only one hot band corresponding to the 1→0 transition (band 1), but two hot bands corresponding to the 1→1 transition (bands 3 and 4). However, this is readily explained, since for the $^2A_1'$ state

the vibrationless level is of $^2A_1'$ symmetry while the n=1 level is of $^2E'$ symmetry. The origin of bands 1 and 3 is the $^2E'$ vibronic level of the ground state. Here the separation between 2 and 1 is the same as the separation between 3 and 5 and places the $^2E'$ vibronic level of the ground state at 100. cm^{-1} above the lowest vibrational level. Similarly the origin of band 4 is the $^2A_1'$ or $^2A_2'$ level which is $15cm^{-1}$ above the lowest vibrational level based on the separation between 5 and 4. The $1 \rightarrow 0$ hot band is absent, because transitions from the $^2A_1'$ or $^2A_2'$ level to the vibrationless level of the upper state are not allowed. The one remaining question is why there would be considerable anharmonicity in the upper state levels. From Fig. 1 one sees that a very large anharmonicity is present in the $^2B_2$ component of the ground state for the bending mode. This results from the low-lying linear configuration. A similar effect is expected for the positive ion, and thus anharmonicity in the bending modes of the upper state would not be surprising.

If the ionization potential of Cu_3 were accurately known experimentally, it would be easier to calculate the excitation energies of the Rydberg states. The best procedure here is to compute energy differences between the ion and the Rydberg states, since one expects very little differential correlation error in this separation. Unfortunately, for Cu_3 the I. P. has only been bracketed as $4.98 < \text{I. P.} < 5.98$ by use of diffferent lasers and observing whether ionization occurs[7]. Thus, we had to compute the ground state ionization potential by SCF plus singles and doubles CI for the ion and neutral states. The result is 4.90 eV for vertical excitation at an equilateral triangle geometry with R Cu-Cu = 4.60 a_0 and 4.97eV for abiabatic excitation (i. e. including the Jahn-Teller stabilization of

the lower state). Thus, our calculation indicates that the I. P. of Cu_3 can not be much larger than 4.98 eV. An alternative way to get the ionization potential is as the experimental excitation energy to the $^2A_1'$ state plus the computed ionization potential of the $^2A_1'$ state. This gives 5.10 eV in reasonable agreement with the value above.

Finally, checks were made of the diffuse basis sets for Cu_3. Here we compared the orbital energy spectrum from a Cu_3^+ calculation for the three basis sets used. The maximum difference in orbital energy was for the $3sa_1'$ orbital which was deeper by 0.04 eV and 0.06 eV, respectively, for the diffuse(2) and diffuse(3) basis sets, as compared to the diffuse(1) basis set. These results indicate that the diffuse portion of the basis set is adequate to describe these states to better than 0.1 eV.

V. Conclusions.

In this paper we report the results of SCF/SDCI calculations for i)selected portions of the ground state surface of Cu_3 ii) for the ionization potential of Cu_3 and iii)for vertical excitation energies for six low-lying excited states.

We find the bonding in this molecule to involve the 4s electrons of the $4s^13d^{10}$ configuration of the Cu atom. The 3d electrons are not inert, however, and correlation of the 3d shell leads to significant bond contraction effects.

The ground state of Cu_3 is found to be a $^2E'$ state arising from $4sa_1'^2 4se'^1$. A linear $^2\Sigma_u^+$ state is found to be 0.26 eV higher. The $^2E'$ state exhibits strong Jahn-Teller distortion, leading to $^2A_1$ (acute angle) and $^2B_2$ (obtuse angle) minima in C_{2v} symmetry. Here the $^2B_2$ minimum is a true minimum on the surface while the $^2A_1$ minimum is a saddle point connecting adjacent $^2B_2$ minima. These calculations lead to a calculated

well depth (energy lowering for Jahn-Teller distortion of the ^2E state to the $^2B_2$ minimum) of 555 cm^{-1} and barrier to pseudorotation (difference in energy between the $^2B_2$ minimum and the $^2A_1$ saddle point) of 171 cm^{-1}. From analysis of the hot bands in the experimental spectrum, Morse, Hopkins, Langridge-Smith, and Smalley[7] conclude that the $^2A_1'$ and $^2A_2'$ levels are 15 cm^{-1} above the vibrationless level of the ground state, while the $^2E'$ level is 100 cm^{-1} above the vibrationless level of the ground state. These experimental vibrational levels are consistent with a strongly Jahn-Teller distorted e' vibrational level of a $^2E'$ electronic state.

The $^2B_2$ minimum is also consistent with the oberved ESR spectrum of Cu_3 in a matrix, which has been interpreted as an obtuse angle structure with most of the radical orbital density on the end Cu atoms. A $^2A_1$ state, on the other hand, would have a large density on the center Cu atom, and would not be consistent with the experiment.

The positive ion of Cu_3 is $^1A_1'$ arising from $4sa_1'^2$. The best estimate of the ionization potential is 5.10 eV based on the experimental excitation energy to the $^2A_1'$ state and the computed I.P. of this state. Experimentally this quantity is not well known but has been bracketed to be greater than 4.98 eV and less than 5.98 eV. The calculated symmetric stretch frequency is 208 cm^{-1} for Cu_3 and 214 cm^{-1} for Cu_3^+.

The low-lying excited states of Cu_3 have the character of Rydberg states and require diffuse basis functions for their description. The upper state in the transition observed by Morse et. al.[7] at 2.3 eV has been assigned as $^2E''$ based on i) significant anharmonicity in the upper state vibrational levels which can be fit by assuming a weakly Jahn-Teller distorted

upper state and ii) observation of selection rules prohibiting the radiative coupling of the $^2A_1'$ and $^2A_2'$ vibronic levels of the ground state with the vibrationless level of the upper state. However, based on the calculated vertical excitation energies we assign the upper state as $^2A_1'$. This assignment is also consistent with the observed vibronic selection rules. The presence of anharmonicity for at least the bending modes of this state is expected due to a low-lying linear configuration which leads to observed large anharmonicity in the $^2B_2$ component of the Jahn-Teller distorted ground state.

ACKNOWLEDGMENTS.

S. P. Walch was supported by a NASA grant(NCC2-296). B. C. Laskowski was supported by NASA under contract NAS2-11922. We would like to acknowledge helpful discussions with Steve Langhoff and Paul Bagus.

REFERENCES

1. W. Weltner,Jr., and R.J. VanZee, Ann. Rev. Phys. Chem., **35**, 291 (1984).
2. See articles in "Recent Developments and Applications of Multi Configuration Hartree-Fock Methods" NRCC Proceedings No. 10, M. Dupuis, editor, NRCC, 1981.
3. P. E. M. Siegbahn, A. Heiberg, B. O. Roos, and B. Levy, Physica Scripta, **21**, 323 (1980); B. O. Roos, P. R. Taylor, P. E. M. Siegbahn, Chem. Phys, **48**, 157 (1980); P. E. M. Siegbahn, J. Almlof, A. Heiberg, and B. O. Roos, J. Chem. Phys., **74**, 2381 (1981).
4. H. Lischka,R. Shepard,F.B. Brown, and I. Shavitt, Int. J. Quantum Chem. Symp. **15**, 91 (1981); P. E. M. Siegbahn, J. Chem. Phys, **72**, 1647 (1980); B. Liu and M. Yoshimine, J. Chem. Phys., **74**, 612 (1981);P. Saxe,D. Fox, H.F. Schaefer III, and N.C. Handy, J. Chem. Phys., **77**,5584(1982).
5. W.A. Goddard,III, T.H. Dunning,Jr., W.J. Hunt, and P.J. Hay, Acc. Chem. Res., **6**, 368 (1973);T.H. Dunning,Jr., in "Advanced Theories and Computational Approaches to the Electronic Structure of Molecules", edited by C.E. Dykstra, Reidel Publishing(1983), p.67
6. L.B. Knight,Jr., R.W. Woodward, R.J. VanZee, and W. Weltner,Jr., J. Chem. Phys, **79**, 5820 (1983).
7. M.D. Morse, J.B. Hopkins, P.R.R. Langridge-Smith, and R.E. Smalley, J. Chem. Phys, **79**, 5316 (1983).
8. C. Backmann, J. Demuynck, and A. Viellard, Faraday Symp. Chem. Soc., **14**, 170 (1980); J. Demuynck, M. Rohmer, A. Strich, and A. Viellard, J. Chem. Phys. **75**, 3443 (1981)
9. H. Tatawaki, E. Migashi, and T. Nakamura, J. Chem. Phys., **76**, 5073 (1982); E. Miyoshi, H. Tatewaki, and T. Nakamura, J. Chem. Phys., **78**, 815 (1982); E. Miyoshi, H. Tatewaki, and T. Nakamura, Int. J. Quant. Chem., **23**, 1201(1983)
10. G.H. Jeung, M. Pelissier, and J.C. Barthelat, Chem. Phys. Lett., **97**, 369 (1983).
11. S.C. Richtsmeier, J.L. Gole, and D.A. Dixon, Proc. Natl. Acad. Sci. USA, **77**, 5611 (1980); S.C. Richtsmeier, D.A. Dixon, and J.L. Gole, J. Phys. Chem. **86**, 3937 (1982)
12. C.W. Bauschlicher,Jr., S.P. Walch, and P.E.M. Siegbahn, J. Chem. Phys., **76**, 6015 (1982).;C.W. Bauschlicher,Jr., S.P. Walch, and P.E.M. Siegbahn, J. Chem. Phys., 78, 3348 (1983).

13. L. Pauling, J. Chem. Phys., 78, 3346 (1983).
14. S.P. Walch and C.W. Bauschlicher,Jr., in "Comparison of Ab Initio Quantum Chemistry with Experiment", edited by R.J. Bartlett, Reidel Publishing, in press
15. R. Martin, J. Chem. Phys., 78, 5840 (1983).
16. P. Scharf, S. Brode, and R. Ahlrichs, Chem. Phys. Lett., 113, 447 (1985).
17. H. Werner and R.L. Martin, Chem. Phys. Lett., 113, 451 (1985).
18. B.C. Laskowski, S.R. Langhoff, and C.W. Bauschlicher,Jr., to be published.
19. W. Meyer, J. Chem. Phys., 58, 1017 (1973).
20. A.J.H. Wachters, J. Chem. Phys., 58, 4452 (1973). The basis set is the same as Wachters' except that due to an input error the inner 4s function is 0.113030 compared to 0.113303 for Wachters'. Since the exponents are not generally optimized to better than about one percent, this error is of no consequence except if someone were to try to reproduce our energies to a large number of significant figures as a program check.
21. P.J. Hay, J. Chem. Phys., 66, 4377 (1977).
22. A.D. McLean and B. Liu, Chem. Phys. Lett., 101, 144 (1983).
23. S.P. Walch, C.W. Bauschlicher,Jr., B.O. Roos, and C.J. Nelin, Chem. Phys. Lett., 103, 175 (1983).
24. R.F. Stewart, J. Chem. Phys., 52, 431 (1970).
25. J. Almlof, MOLECULE, a gaussian integral program.
26. S.R. Langhoff and E.R. Davidson, Intern. J. Quantum Chem., 8, 61(1974)
27. P.E.M. Seigbahn, C.W. Bauschlicher,Jr., B. Roos, A. Hieberg, P. R. Taylor, and J. Almof, SWEDEN, a vectorized SCF MCSCF direct CI.
28. D.P. DiLella, K.V. Taylor, and M. Moskovits, J. Phys. Chem., 87, 524(1983)
29. G. Herzberg,"Molecular Spectra and Molecular Structure III. Electronic Spectra and Electronic Structure of Polyatomic Molecules", Reinhold, 1966
30. J.A. Howard, K.F. Preston, R. Sutcliffe, and B. Mile, J. Phys. Chem., 87, 536 (1983).
31. K. Kernisant, G.A. Thompson, and D.M. Lindsay, J. Chem. Phys., 82, 4739 (1985).
32. K.P. Huber and G. Herzberg,"Molecular Spectra and Molecular Structure IV. Constants of Diatomic Molecules", Reinhold, 1979
33. H. Hilpert and K. A. Gingerich, Ber. Bunsenges Phys. Chem., 84, 739 (1980).
34. W.J. Hunt and W.A. Goddard III, Chem. Phys. Lett., 3, 414 (1969).
35. S.P. Walch and W.A. Goddard III, Surface Science, 72, 645 (1978).

Table Ia. Energies for Cu_3 (Equilateral Triangle Geometries)

R(Cu-Cu)	E(SCF)	E(CI)
4.25	-4916.44765	-4917.06800
4.50	-4916.46241	-4917.07585
4.75	-4916.46806	-4917.07484
5.00	-4916.46856	-4917.06914

Table IB. Energies for Cu_3^+ (Equilateral Triangle Geometries)

R(Cu-Cu)	E(SCF)	E(CI)
4.25	-4916.29195	-4916.88681
4.50	-4916.30746	-4916.89562
4.60	-4916.31072	-4916.89631
4.75	-4916.31342	-4916.89531
5.00	-4916.31382	-4916.88999

Table II. Energies for Cu_3 $^2A_1$ (Bent Geometries, R(Cu-Cu)=4.60)

Cu-Cu-Cu angle	E(SCF)	E(CI)
50.0	-4916.44842	-4917.06624
55.0	-4916.46280	-4917.07700
58.0	-4916.46528	-4917.07734
60.0	-4916.46549	-4917.07622
70.0	-4916.45808	-4917.06361
80.0	-4916.44562	----------

Table III. Energies for Cu_3 $^2B_2$ (Bent Geometries, R(Cu-Cu)=4.60)

Cu-Cu-Cu angle	E(SCF)	E(CI)
50.0	-4916.43485	----------
55.0	-4916.45595	-4917.06988
60.0	-4916.46538	-4917.07634
65.0	-4916.46965	-4917.07802
70.0	-4916.47153	-4917.07781
80.0	-4916.47235	-4917.07587
90.0	-4916.47198	-4917.07406

Table IV. Energies for Cu_3 (Linear Geometries)

R(Cu-Cu)	E(SCF)	E(CI)
4.30	-4916.46000	-4917.06744
4.60	-4916.46819	-4917.06943
4.90	-4916.46895	-4917.06443

Table V. Geometry Optimization for Cu_3 $^2A_1$

R_1	R_2	E(SCF)	E(CI)
4.60	4.60	-4916.46599	-4917.07622
4.75	4.60	-4916.46869	-4917.07681
4.90	4.60	-4916.47076	-4917.07627
4.60	4.248	-4916.46280	-4917.07700
4.60	4.460	-4916.46528	-4917.07734
4.75	4.30	-4916.46682	-4917.07790
4.753	4.383		-4917.07809[a]

[a] Predicted minimum from the above six points.

Table VI. Geometry Optimization for Cu_3 $^2B_2$

R_1	R_2	E(SCF)	E(CI)
4.60	4.60	-4916.46538	-4917.07634
4.60	4.943	-4916.46965	-4917.07802
4.60	5.277	-4916.47153	-4917.07781
4.50	4.943	-4916.46855	-4917.07876
4.40	4.943	-4916.46647	-4917.07858
4.47	5.03	-4916.46891	-4917.07886
4.474	5.035		-4917.07887[a]

[a] Predicted minimum from the above six points.

Table VII. Radical Orbital Mulliken Populations

	$^2A_1$		$^2B_2$	
	Center	End	Center	End
s	.63237	.22106	.00000	.83775
p	.00272	.14392	.11584	.04641
d	.00103	.00096	.00092	.00093

Table VIII. Calculated Vertical Excitation Energies for Cu_3.

State Sym.	Valence CI	SDCI
$^2E'$ ($3pe'$)	2.92	
$^2A_1'$ ($3da_1'$)	2.88	
$^2E''$ ($3de''$)	2.80	3.32
$^2E'$ ($3de'$)	2.14	
$^2A_1'$ ($3sa_1'$)	1.79	2.14
$^2A_2''$ ($2pa_2''$)	1.06	1.25
$^2E'$ ($2pe'$)	0.00	0.00

Table IX. Energies for Cu_3 $^2\Delta$ State (Linear Geometries)

R(Cu-Cu)	E(SCF)	E(CI)
4.30	-4916.44501	-4917.01655
4.60	-4916.45574	-4917.01898
4.90	-4916.45630	-4917.01226

Figure 1. Calculated bending curves for two C_2v cuts through the ground state potential surface of Cu_3. Two sides are fixed at R Cu-Cu = 4.60 a_0 and the Cu-Cu-Cu angle is varied.

Figure 2. The vibronic levels for an e′ vibration of a $^2E'$ molecule with D_{3h} symmetry for i)a symmetric state and ii) a strongly Jahn-Teller distorted state (from Ref. 29). The locations of the vibronic levels for the Jahn-Teller distorted state correspond to the observed ground state vibronic levels for Cu_3 derived from the spectroscopic studies of Morse, Hopkins, Langridge-Smith, and Smalley (Ref. 7).

Figure 3. Contour plots for selected valence and Rydberg orbitals of Cu_3. Solid lines indicate positive contours, dotted lines indicate negative contours, and nodal surfaces are indicated by dashed lines.

Figure 4. The experimental spectrum of Cu_3 observed by Morse, Hopkins, Langridge-Smith, and Smalley(Ref. 7).

Fig 1

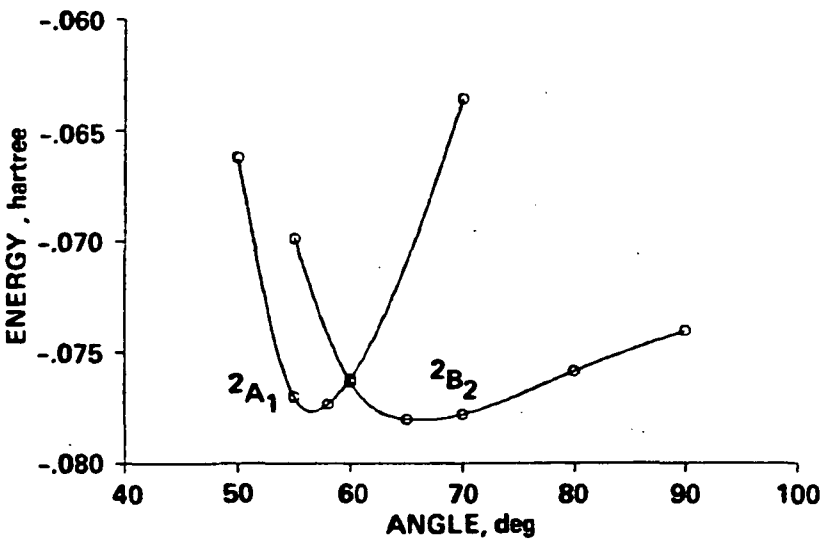
-.060
-.065
-.070
-.075
-.080
ENERGY , hartree
40
50
60
70
80
90
100
ANGLE, deg
$^2A_1$
$^2B_2$

Fig. 2

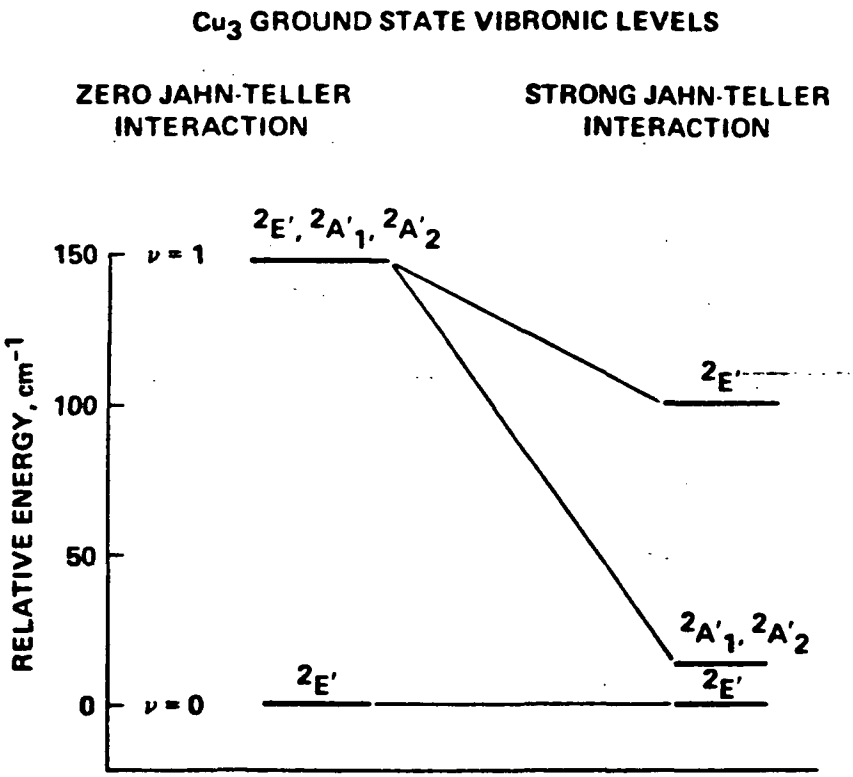
Cu3 GROUND STATE VIBRONIC LEVELS
ZERO JAHN-TELLER INTERACTION
STRONG JAHN-TELLER INTERACTION
RELATIVE ENERGY, cm-1
150
100
50
0
ν = 1
ν = 0
2E', 2A'1, 2A'2
2E'
2A'1, 2A'2
2E'
2E'

Selected Orbitals for Cu_3

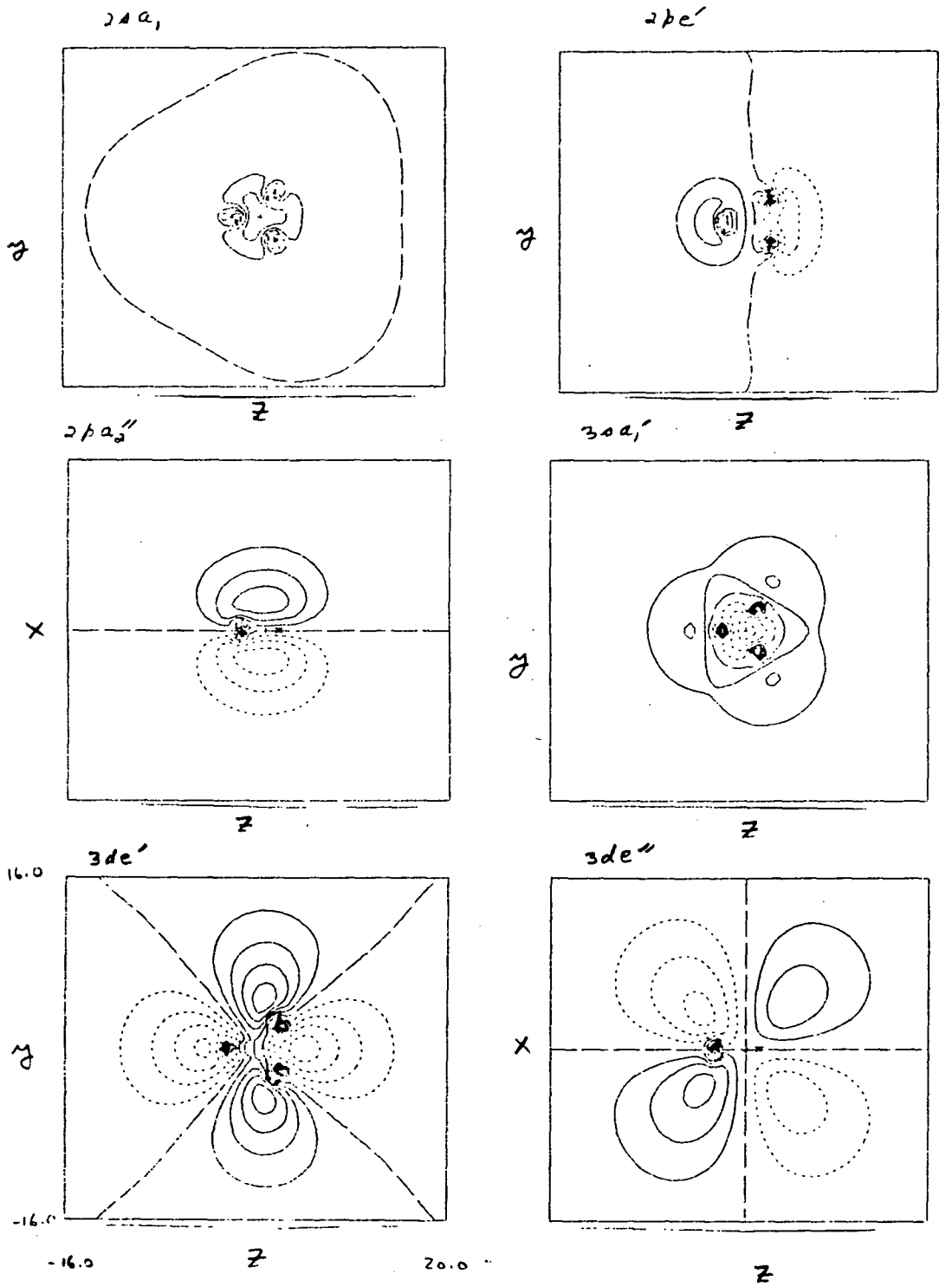

Fig. 4

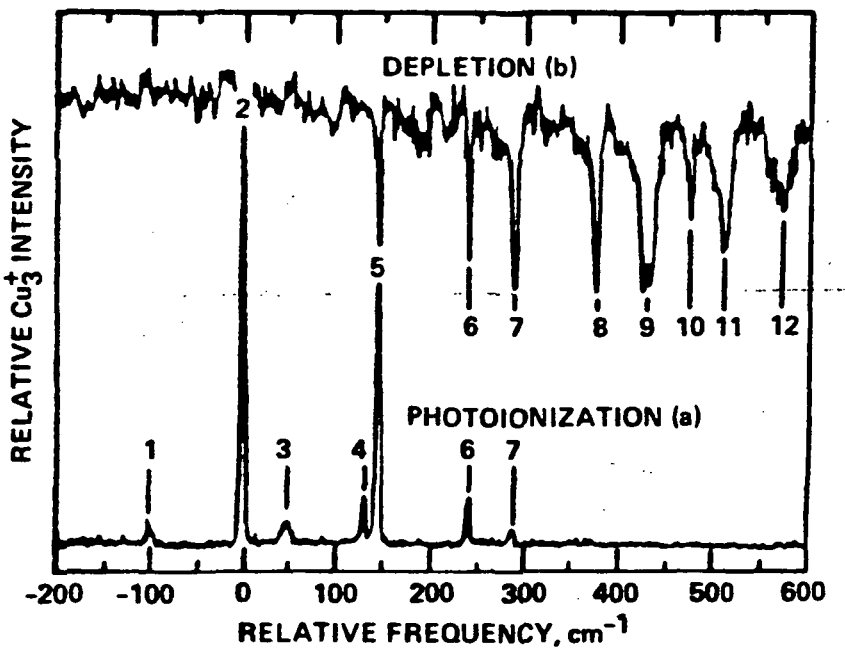
DEPLETION (b)
PHOTOIONIZATION (a)
RELATIVE Cu_3^+ INTENSITY
RELATIVE FREQUENCY, cm^{-1}
1
2
3
4
5
6
7
8
9
10
11
12
-200
-100
0
100
200
300
400
500
600